Locked in the icehouse : evolution of an endemic Epimeria (Amphipoda, Crustacea) species flock on the Antarctic shelf

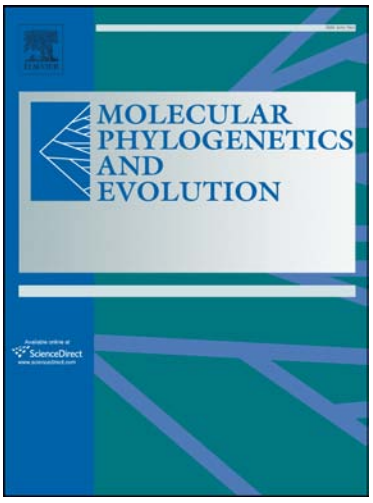

Locked in the icehouse: evolution of an endemic *Epimeria* (Amphipoda, Crustacea) species flock on the Antarctic shelf

Marie L. Verheye, Thierry Backeljau, Cédric d'Udekem d'Acoz

PII: S1055-7903(16)30436-5
DOI: http://dx.doi.org/10.1016/j.ympev.2017.05.013
Reference: YMPEV 5826

To appear in: *Molecular Phylogenetics and Evolution*

Received Date: 10 January 2017
Revised Date: 12 May 2017
Accepted Date: 14 May 2017

Please cite this article as: Verheye, M.L., Backeljau, T., d'Udekem d'Acoz, C., Locked in the icehouse: evolution of an endemic *Epimeria* (Amphipoda, Crustacea) species flock on the Antarctic shelf, *Molecular Phylogenetics and Evolution* (2017), doi: http://dx.doi.org/10.1016/j.ympev.2017.05.013

Locked in the icehouse: evolution of an endemic *Epimeria* (Amphipoda, Crustacea) species flock on the Antarctic shelf

Marie L. Verheye[a,b], Thierry Backeljau[a,c], Cédric d'Udekem d'Acoz[a]

[a] Royal Belgian Institute of Natural Sciences, OD Taxonomy and Phylogeny, rue Vautier 29, 1000 Brussels, Belgium

[b] Catholic University of Louvain-la-Neuve,Department of Biology, Marine Biology Laboratory, Croix du Sud 3 bte L7.06.04, 1348 Louvain-la-Neuve, Belgium

[c] University of Antwerp, Evolutionary Ecology Group, Universiteitsplein 1, 2160 Antwerp, Belgium

Corresponding author: M. Verheye

E-mail: marie.verheye@naturalsciences.be

Phone : +32 (0)2 627 44 57

Abstract

The Antarctic shelf's marine biodiversity has been greatly influenced by the climatic and glacial history of the region. Extreme temperature changes led to the extinction of some lineages, while others adapted and flourished. The amphipod genus *Epimeria* is an example of the latter, being particularly diverse in the Antarctic region. By reconstructing a time-calibrated phylogeny based on mitochondrial (COI) and nuclear (28S and H3) markers and including *Epimeria* species from all oceans, this study provides a temporal and geographical framework for the evolution of Antarctic *Epimeria*. The monophyly of this genus is not supported by Bayesian Inference, as Antarctic and non-Antarctic *Epimeria* form two distinct well-supported clades, with Antarctic *Epimeria* being a sister clade to two stilipedid species. The monophyly of Antarctic *Epimeria* suggests that this clade evolved in isolation since its origin. While the precise timing of this origin remains unclear, it is inferred that the Antarctic lineage arose from a late Gondwanan ancestor and hence did not colonize the Antarctic region

after the continent broke apart from the other fragments of Gondwanaland. The initial diversification of the clade occurred 38.04 Ma (95 % HPD [48.46 Ma; 28.36 Ma]) in a cooling environment. Adaptation to cold waters, along with the extinction of cold-intolerant taxa and resulting ecological opportunities, likely led to the successful diversification of *Epimeria* on the Antarctic shelf. However, there was neither evidence of a rapid lineage diversification early in the clade's history, nor of any shifts in diversification rates induced by glacial cycles. This suggests that a high turnover rate on the repeatedly scoured Antarctic shelf could have masked potential signals of diversification bursts.

Keywords

Amphipoda – Southern Ocean – Historical Biogeography – Phylogeny – Divergence times – Diversification[1]

1. Introduction

The Southern Ocean is traditionally viewed as an isolated ecosystem where the marine fauna has essentially evolved *in situ* (Clarke and Crame, 1989; Dell, 1972; Knox and Lowry, 1977; Lipps and Hickman, 1982). The eastward flowing Antarctic Circumpolar Current (ACC), encircling Antarctica since the Oligocene, is the most powerful sea current on Earth. The Antarctic Polar Front (APF), one of the ACC's jets, marks a sharp change in surface water temperatures and impedes north-south exchange of water. Therefore, it appears to be an important barrier to dispersal (Angel, 1997; Clarke et al., 2005; Dell, 1972). The high degree of species-level endemism of the Antarctic marine fauna is a signature of this long history in isolation (Arntz et al., 1997; Clarke and Crame, 1997; Clarke and Johnston, 2003). Some Antarctic lineages are descendants of Gondwanan ancestors, which arose by vicariance when the supercontinent progressively broke apart (e.g. Brandt, 1992; Clarke and Johnston, 1996; Waters et al., 2007; Williams et al., 2003). While the APF has been

[1] ACC = Antarctic circumpolar current ; APF = Antarctic Polar Front ; MMCT = Mid-Miocene climate transition ; COI = cytochrome b oxidase subunit I ; H3 = histone 3 ; BI = Bayesian Inference ; ILD = Incongruence Length Difference test ; ML = Maximum Likelihood ; BIC = Bayesian Information criterion ; PP = posterior probability ; BV = bootstrap value ; MOTU = molecular taxonomic unit ; MCMC = Markov chain Monte-Carlo ; UCLD = uncorrelated lognormal distribution ; UCED = uncorrelated exponential distribution ; BF = Bayes Factor ; SD = standard deviation ; LTT = lineage through time plot ; PB = Pure Birth ; BD = Birth-Death ; AIC = Akaike Information criterion ; DDL = density-dependent linear ; DDX = density-dependent exponential ; BDS = Birth-Death Shift ; dAIC = difference of AIC ; wAIC = Akaike weight ; MLE = marginal likelihood estimate ; MRCA = most recent common ancestor ; BAMM = Bayesian analysis of macroevolutionary mixtures ; MAP = maximum posterior probability ; HPD = higher posterior density ; EECO = early Eocene climate optimum ; EOCT = Ecocene-Oligocene climate transition

shown to be a permeable barrier for a variety of pelagic and deep-sea organisms (Antezana, 1999; Bargelloni et al., 2000; Brandt et al., 2007; Hodgson et al., 1997; Page and Linse, 2002; Pawlowski et al., 2007; Thatje and Fuentes, 2003), the Drake Passage is too deep to allow the dispersal of stenobathic shelf organisms along the benthos (e.g. Hunter and Halanych, 2008; Shaw et al., 2004). However, some benthic taxa lacking a pelagic stage may be able to cross the front by drifting on macroalgae or floating debris (Barber et al., 1959; Coombs and Landis, 1966; Fraser et al., 2009; Helmuth et al., 1994; Waters, 2008). Historical cases of polar emergences — colonizations of the Antarctic shelf from the depths —or submergences — dispersals from the shelf towards the depths — were also inferred for some strictly benthic organisms (Held, 2000; Strugnell et al., 2008). Such movements may be facilitated by the formation of cold and dense water near the continent which sinks northward at a layer below 4000 m depth to become the "Antarctic Bottom Water", thereby forming an isothermal water column between the shelf and the deep-sea (Knox and Lowry, 1977). The Southern Ocean fauna therefore contains a mixture of lineages with different histories, some have evolved *in situ* since before Antarctica existed, others are more recent colonizers (Clarke and Crame, 1989).

All along its geological history, the Antarctic region has faced profound climatic changes, which deeply impacted Southern Ocean marine biodiversity (Clarke and Crame, 1997). The fossil record indicates major changes in the nature of the marine fauna along the cooling trend, which began across the early to middle Eocene boundary (ca. 48-49 Ma). While many taxa went extinct, the availability of previously occupied benthic niches provided ecological opportunities for surviving lineages (Aronson et al., 2007; Brandt, 1999). Ecological opportunity has been inferred to drive initial rapid lineage diversification (Condamine et al., 2013; Losos and Mahler, 2010; Yoder et al., 2010). As lineages rapidly fill unoccupied niches and available habitats run out, the rate of diversification would consequently decrease (Freckleton and Harvey, 2006; Rabosky and Lovette, 2008; Schluter, 2000; Walker and Valentine, 1984). Alternatively, the simultaneous formation of multiple geographical barriers can be responsible for a burst of allopatric speciation (Rundell and Price, 2009). Hence, by providing ecological opportunities or causing allopatric speciation, several main events in Antarctica's climatic history could have impacted species' origination rates. For instance, the gradual extinction of decapods, possibly beginning with the cooling trend which started in the early Eocene (Thatje et al., 2005), likely triggered the radiation of the peracarids (Aronson et al., 2007). The Eocene-Oligocene boundary (34 Ma) was marked by a sudden drop in temperatures, the first continent-wide glaciations (Lear et al., 2000, 2004), the opening of the Tasmanian and Drake passages (Barker, 2001; De Broyer and Jażdżewska, 2014; Exon et al., 2000; Stickley et al., 2004) and the formation of the ACC (Lawver and Gahagan, 2003; Lyle et al., 2007; Pfuhl and McCave, 2005). The resulting thermal and geographical isolation of the Antarctic region is presumed to have promoted vicariant speciations in Southern

Ocean taxa. Since the Mid-Miocene Climate Transition (MMCT; ~14 Ma), the ice-shelf grounding line periodically extended to the outer shelf break, at least in some places during glacial maxima. These glacial cycles, which intensified in the Late Pliocene-Pleistocene period (Lewis et al., 2008; McKay et al., 2012; Pollard and DeConto, 2009) were inferred to act as a "diversity pump" on the Southern Ocean continental shelf (Clarke and Crame, 1989, 2010; Clarke et al., 1992). The isolation of populations in ice-free refugia during glacial advances would have resulted in allopatric speciations of less dispersive organisms (Thatje et al., 2005).

The Antarctic component of the amphipod genus *Epimeria* (Costa, 1851) was put forward as an example of an Antarctic species flock, i.e. a highly diverse clade of species that originated and diversified in the Antarctic region (Lecointre et al., 2013). However, the assumption of monophyly was based on a previous COI phylogeny of *Epimeria*, comprising 17 Antarctic species, but only two non-Antarctic (New Zealand) species (Lörz et al., 2009). Yet, the genus is cosmopolitan, but particularly well represented in the Southern Ocean, with 26 described species out of a total of 54 worldwide (Coleman, 2007; Lörz, 2009; Lörz et al., 2007, 2009, 2011). Moreover, a recent study of COI and 28S sequence data identified 24 lineages as putative new Antarctic species, showing that the species richness of this genus on the shelf is still greatly underestimated (Verheye et al., 2016). *Epimeria* contains a mixture of regionally-restricted and (almost) circum-Antarctic species (d'Udekem d'Acoz and Verheye, *in press*; Verheye et al., 2016), but no species are found on both sides of the APF. Their mostly benthic (only two pelagic species are known) and brooding ecology, coupled with limited eurybathy, would prevent such long-distance dispersal across deep passages, on ecological timescales (d'Udekem d'Acoz and Verheye, *in press*). In the COI phylogeny of Lörz and Held (2004), comprising six Antarctic and no extralimital species, ages of 15.7 and 34.9 Ma were inferred for the last common ancestor of Antarctic *Epimeria*, using respectively a COI rate of evolution estimated for cirripeds and for alpheid shrimps, and assuming a strict molecular clock. The authors concluded that Southern Ocean *Epimeria* evolved *in situ* when Antarctica was already isolated from the other fragments of Gondwana (Lörz and Held, 2004). The cosmopolitan distribution of *Epimeria,* coupled with a low dispersal potential, makes it a good model to study the connection between the Antarctic shelf and the other oceans, the origin of this component of the shelf benthos and its *in situ* diversification patterns.

Inferences on the historical biogeography of the *Epimeria* Antarctic shelf species are not possible without a robust phylogeny, based on an extensive sampling of both Antarctic and non-Antarctic species. Therefore, we reconstructed a phylogeny of *Epimeria* using three gene fragments (COI, 28S and H3)

and including 12 out of the 26 described Antarctic *Epimeria* species as well as 24 putative new Antarctic *Epimeria* species. The non-Antarctic material is composed of 21 *Epimeria* species collected in every other world's oceans. In order to explore the monophyly and systematics of *Epimeria*, we included representatives of other families which form a clade with *Epimeria*, viz. Acanthonotozomellidae, Dikwidae, Stilipedidae and Vicmusiidae (Verheye et al., 2015). Then, we used a relaxed molecular clock to date the phylogenetic tree and considered the geographical distribution of the specimens to address the following issues: 1. Does the Antarctic component of *Epimeria* form a single clade or does the phylogeny provide evidence of historical dispersal events in and/or out of the shelf (which would make this Antarctic component non-monophyletic)? 2. When and where did the Antarctic component originate i.e. is it a Gondwanan relict or a more recent colonizer? and 3. Does the historical diversification pattern of Antarctic *Epimeria* bear signatures of an early diversification burst, or of shifts in diversification rates which might be associated with climatic events (e.g. glacial cycles)?

2. Material and Methods

2.1. Taxon sampling

We included data of 12 out of the 26 described species of Antarctic *Epimeria*, as well as the 24 putative new Antarctic species of Verheye et al. (2016), i.e. a total of 36 out of 50 known species (72.5 %). Non-Antarctic *Epimeria* included one species from continental Norway (*Epimeria cornigera*), one from the Svalbard Archipelago (*Epimeria loricata*), one from Mexico (*Epimeria morronei*) and 16 putative new species, viz. 14 from the Melanesian subregion (Indonesia, Papua New Guinea, New Caledonia, Solomon, Vanuatu and Fiji islands), one from Taiwan and one from Mozambique. Species from other families that were shown to be related to *Epimeria* in Verheye et al. (2015) (i.e. *Acanthonotozomoides oatesi* and Acanthonotozomellidae n. gen. n. sp. [Acanthonotozomellidae], *Dikwa andresi* [Dikwidae], *Astyra abyssi*, *Bathypanoploea schellenbergi* and *Alexandrella dentata* [Stilipedidae], and *Acanthonotozomopsis pushkini* [Vicmusiidae]) were included as well, in order to explore the monophyly of the genus. Three iphimediid species were used as outgroup. All specimens used in this study are listed in Table 1.

Samples were collected during several expeditions of the R.V. Polarstern in the Southern Ocean: ANT-XXIV/2, ANTXXIII/8, ANT-XXVII/3 and ANT-XXIX/3 in the Drake Passage, Bransfield Strait, eastern coast of the Antarctic Peninsula and eastern Weddell Sea. Additional specimens were sampled from the Adélie

Coast during the CEAMARC and REVOLTA I, II, III expeditions and in Prydz Bay during the MD42 (SIBEX) expedition of the R.V. Marion Dufresne. One specimen was sampled during the JR144 expedition with the RRS James Clark Ross near Elephant Island. Non-Antarctic specimens were sampled during BIOPAPUA, Papua Niugini (Papua New Guinea), KARUBAR (Indonesia), EXBODI, NORFOLK2, BATHUS3 (New Caledonia), SOLOMON2 and 3 (Solomon Islands), MUSORSTOM8, SANTO (Vanuatu), FIDJI (Fiji Islands), Taiwan 2000 (Taiwan) and MAINBAZA (Mozambique) expeditions. Additional material was obtained by opportunistic collections from Mexico and Norway (including the Svalbard archipelago) (Table 1).

All specimens were preserved in 96–100% ethanol for DNA analysis. Vouchers are deposited at the Royal Belgian Institute of Natural Sciences (RBINS, Brussels, Belgium) and the Muséum National d'Histoire Naturelle (MNHN, Paris, France). For voucher collection ID numbers, see Table 1.

2.2. DNA sequencing

DNA was extracted from the pleopods and abdomen muscles using a NucleoSpin® Tissue kit (Macherey-Nagel) following the manufacturer's protocol for animal tissues. The DNA was eluted in 100 µl of sterile distilled H_2O (RNase free) and stored at -20 °C.

Partial segments of the mitochondrial cytochrome c oxidase subunit I (COI) (~550 bp), nuclear 28S rDNA (~1400 bp) and Histone 3 (H3) (~360 bp) were amplified by PCR. Amplifications were performed in a 25 µl reaction mix, which contained 0.15 µl Taq DNA Polymerase (5 U μl^{-1}; Qiagen, Antwerpen, Belgium), 2.5 µl 10x CoralLoad PCR Buffer (Qiagen, Antwerpen, Belgium), 2.5 µl dNTPs mix (250 µM of each), 11–16 µl RNase-free water, 1.25 µl of each primer (2 µM), and 1–6 µl of DNA extract. The COI fragment was amplified using the primers Cp-COIF3 (Pilar Cabezas et al., 2013) and COI2R (Otto and Wilson, 2001). The thermal cycling used for the COI amplification followed Pilar Cabezas et al. (2013), except for the annealing temperature set at 51°C. The 28S rDNA fragment was amplified using the primers 28S-3311F (Witt et al., 2006) and 28R (Hou et al., 2007), modified as follows: 5'-GGGACTACCCGCTGAACTTAAGCAT-3' and 5'-GTCTTTCGCCCCTATGCCCAACTG-3'. PCR amplification settings for 28S rDNA consisted of an initial denaturation for 3 min at 94 °C, followed by 40 cycles of denaturation at 94 °C for 40 s, annealing at 45 °C for 40 s, extension at 72 °C for 90 s, and a final extension at 72 °C for 10 min. The H3 fragment was amplified using the primers H_3aF and H_3aR (Colgan et al., 1998). PCR amplification settings were as in Colgan et al. (1998), with an annealing temperature of 54–60°C.

The PCR products were visualized under blue light on 1.2 % agarose gel stained with SYBR Safe (ThermoFisherScientific, Waltham, MA, USA), with a comigrating 200-bp ladder molecular-weight marker to confirm their correct amplification. Prior to sequencing, PCR products were purified using Exonuclease I (20 U μl^{-1}) and FastAP^{TM} Thermosensitive alkaline phosphatase (1 U μl^{-1}) (ThermoFisher Scientific, Waltham, MA, USA), following the manufacturer's protocol. Forward and reverse strands were sequenced with fluorescent-labeled dideoxynucleotide terminators (BigDye v.3.1; Applied Biosystems, Foster City, CA, USA) following the protocol of Sanger et al. (1977) and using an automated ABI 3130xl DNA analyzer (Applied Biosystems, Foster City, CA, USA). Both fragments were sequenced using the PCR primers.

2.3. Phylogenetic analyses

Sequence chromatograms were checked, and forward and reverse sequence fragments were assembled using Codoncode Aligner v.3.7.1. (CodonCode Corporation; http://www.codoncode.com/aligner/). All sequences have been deposited in GenBank (Table 1).

28S sequences were aligned with MAFFT v.7 (Katoh and Standley, 2013) (http://mafft.cbrc.jp/alignment/server/), using the structural alignment strategy Q-INS-i under default settings. As some regions of the 28S sequences were too divergent to be confidently aligned, the software program Aliscore v.2.0. (Misof and Misof, 2009) was used to identify poorly aligned regions for removal with Alicut v.2.3, prior to further analysis. CLUSTALW was used to align the COI and H3 sequences in MEGA6 (Tamura et al., 2013). In order to prevent inclusion of pseudogenes in the analyses, amino acid translations of both fragments were checked for stop codons.

In order to evaluate the congruence between genes and reconstruction methods, preliminary phylogenetic trees were inferred using Bayesian inference (BI) on the separate datasets. The Incongruence Length Difference (ILD) test (Farris et al., 1995) was implemented using Paup*4.0b10 (Swofford, 2003). BI and Maximum Likelihood (ML) were then used to reconstruct phylogenetic relationships based on a dataset concatenated with SequenceMatrix (Vaidya et al., 2011).

The best-fit models of DNA substitution were selected using the Bayesian Information Criterion (BIC) on the concatenated dataset partitioned by gene and by codon position (for COI and H3), in PartitionFinder (Lanfear et al., 2012). This model selection procedure was performed both by assuming a single set of underlying branch lengths for the tree and independent set of branch lengths for each partition and the best scheme was selected based on the BIC value.

BI trees were reconstructed using MrBayes v.3.2 (Ronquist and Huelsenbeck, 2003) on the CIPRES portal (Miller et al., 2010). BI analysis of each alignment included two runs of 10^7 generations. Trees were sampled every 1000 generations using four Markov chains, and default heating values. Convergence was assessed by the standard deviation of split-frequencies (<0.01) and by examining the trace plots of log-likelihood scores in Tracer 1.6 (Rambaut and Drummond, 2005). The first 10 % trees were discarded as burn-in, while the remaining trees were used to construct a 50 % majority rule consensus tree and estimate the posterior probabilities (PP). Nodes with posterior probabilities (PP) ≥ 0.95 were considered as significantly supported.

ML trees were estimated using GARLI v.2.0 (Zwickl, 2006). For each dataset, 10 separate ML searches were run independently from different stepwise-reconstructed trees. The best scoring tree across runs was considered for further analyses. Confidence levels of branches were estimated by 1000 bootstrap replicates. Nodes with bootstrap values (BV) ≥ 70 were considered meaningful.

2.4. Estimation of divergence times

As intraspecific variation may lead to the overestimation of divergence times (Ho et al., 2008), the time-calibrated reconstruction was based on a reduced multimarker dataset. For the Antarctic *Epimeria* clade, one individual per Molecular Taxonomic Unit (MOTU) identified as a putative species by Verheye et al. (2016) was retained. For other sequences, one individual per clade corresponding to a morphospecies was selected.

BEAST2 (Bouckaert et al., 2014) on the CIPRES portal (Miller et al., 2010) was used to estimate divergence times under a Bayesian approach. A Bayesian Model Averaging method was implemented in BEAST2 with the bModelTest package (Bouckaert and Drummond, 2015) in order to estimate a phylogeny averaged over site models, and not to rely on a likelihood-based method to determine the site model. During the Bayesian analysis, Markov Chain Monte-

Carlo (MCMC) proposals switch between substitution models and estimate the posterior support for gamma-distributed rate heterogeneity, proportion of invariable sites and unequal base frequencies.

We simultaneously inferred the posterior distribution of trees and estimated divergence times assuming a relaxed clock model of evolution, allowing substitution rates to vary among branches. Both uncorrelated lognormal (UCLD) and exponential (UCED) models of rate change were implemented. In order to assess the pertinence of a relaxed estimation, the coefficients of variation of the clock rates were checked in Tracer v.1.6 (Rambaut et al., 2014). The coefficient of variation is the standard deviation of the clock rate distribution divided by its mean, and is used to assess the clock-likeness of the data. Values closer to zero indicate that the data are more clock-like. Therefore, values < 0.1 are generally considered low enough to justify the use of a strict molecular clock (Drummond and Bouckaert, 2015). To identify the best relaxed clock model, the marginal likelihoods of the competing models were estimated and summarized via the path-sampling method (Lartillot and Philippe, 2006), implemented in the MODEL_SELECTION package in BEAST2. Both Yule and Birth-death speciation processes were used as tree priors in combination with the UCLD clock model, and a path-sampling method was again used to select for the best tree model. All the path-sampling analyses were run for 100 steps of 2×10^6 generations each. The log Bayes Factors (BF) were calculated as follows: $\log_e BF(M_0, M_1) = \log_e P(X|M_0) - \log_e P(X|M_1)$, where $\log_e P(X|M_i)$ is the marginal $\log_e$-likelihood estimate for the model M_i. The strength of support for a given model was based on the interpretation of BF suggested by Kass and Raftery (1995). Values of $2 \log_e BF$ between 0 and 3 were interpreted as no evidence for the alternative model M_1 over the null model M_0. When $2 \log_e BF$ values were above 3, the alternative model M_1 was supported over the null model M_0, and values over 20 were interpreted as a very strong support for the alternative model.

Likely due to their thin cuticle, peracarid crustaceans do not fossilize well (e.g. Briggs and Kear, 1994; Briggs and Wilby, 1996; Taylor, 1972). Their fossil record is very incomplete and therefore of limited utility for molecular dating. The aquatic fossil amphipods known (Coleman and Myers, 2000; Coleman and Ruffo, 2002; Coleman, 2004, 2006; Jażdżewski and Kulicka, 2000a, 2002; Jażdżewski and Kupryjanowicz, 2010; Jażdżewski et al., 2014; McMenamin et al., 2013; Weitschat et al., 2002) are all from freshwater taxa, phylogenetically distant from *Epimeria* (Verheye et al. 2015). Moreover, the detailed phylogenetic placement of these fossils could generally not be determined, due to their relatively poor preservation (e.g. Coleman, 2004; Coleman and Myers, 2000; Coleman and Ruffo, 2002; Jażdżewski and Kulicka, 2000b). Similarly, there is no unambiguous biogeographical event that could be used to calibrate the tree. We therefore used priors on rates of COI, 28S and H3 evolution based on rates inferred in previous studies. The prior rate of COI was set as a normal

distribution with a mean of 0.018 substitutions/site/My and a standard deviation (SD) of 0.0043. This rate was previously inferred for *Pontogammarus* amphipods (Nahavandi et al., 2013). A normal prior with a mean of 0.003 substitutions/site/My and SD of 0.0007 was used for the 28S gene, a rate inferred for the *Gammarus balcanicus* complex (Mamos et al., 2016). Rates of H3 evolution are, to our knowledge, not available for amphipods. Therefore, the prior rate of H3 was set as a normal distribution with a mean of 0.0019 and SD of 0.0004, a rate inferred for freshwater crabs (Klaus et al., 2010).

Two independent runs were performed with 200 million generations and a sampling frequency of 20000 generations. The first 1000 trees were discarded as burn-in and the results of the two runs were combined using the LogCombiner v1.7.5. Convergence was assessed by trace plots in Tracer v.1.6. and the effective sampling size for all parameters was more than 200 (Rambaut et al., 2014). The maximum clade credibility tree showing the mean nodal height was generated by TreeAnnotator v1.8.0. The final analyses were also run without data to ensure that the prior settings will not bias the results.

2.5. Rate and mode of diversification

The reduced dataset (one individual per species or putative species) was also used for diversification rates analyses because intraspecific polymorphisms can induce a false increase in diversification rates in the most recent history. All the diversification rate analyses were based on the Antarctic *Epimeria* clade. Incomplete taxonomic sampling can result in spurious declines in diversification rates over time (Pybus and Harvey, 2000). Our phylogeny comprises 72.5 % of the known (putative) species. However, as Verheye et al. (2016) discovered at least 24 new *Epimeria* species from the Peninsula, eastern Weddell Sea and Adélie Coast, it is likely that similar studies of material from e.g. the Ross, Amundsen and Bellingshausen Seas will reveal an even higher diversity within the genus. Therefore, the methods used herein to examine diversification patterns tested the effect of different levels of taxonomic sampling on the results: sampling proportions of 72 %, 50 % and 10 % were considered.

A mean semilogarithmic lineage through time (LTT) plot was constructed using the R package Ape to visualize the temporal pattern of lineage diversification. A straight line is expected under constant diversification rate. A departure from this straight line in the distant past may indicate a diversification rate change: (1) a concave plot either indicates a decelerating diversification rate or incomplete taxon sampling, (2) a convex plot may indicate accelerating diversification or a non-zero background extinction rate. The command sim.bd.taxa.age from the R package TreeSim (Stadler, 2011) was used to simulate

100 trees under Pure Birth (PB) and Birth-Death (BD), with speciation and extinction rates estimated with bd.shift.optim from the R package TreePar (Stadler, 2011). Both functions were used assuming a sampling fraction of 72 %. The LTT plot of the empirical phylogeny was compared to the 95 % confidence intervals of the expected pattern under PB and BD, to detect eventual deviations from the null hypothesis of constant rates.

In order to account for incomplete taxonomic sampling in methods that do not include a correction for missing species, we used the CorSim function from the R package TreeSim to simulate the missing splits on the empirical phylogeny (Cusimano et al., 2012). Missing speciation events were simulated 200 times under the assumption that evolution followed a constant BD model. Simulated branching times are added to the empirical branching times to obtain 200 completed (semi-empirical) datasets. Speciation and extinction rates used for the simulation were those estimated under BD with the bd.shifts.optim function of the TreePar package. Missing taxa were assumed to be located randomly across the tree, as both deep and shallower nodes are likely missing from the phylogeny. Three semi-empirical datasets were obtained for 72 %, 50 % and 10 % sampling.

The γ statistic was calculated on the semi-empirical datasets, using the GamStat function of the R package LASER (Rabosky, 2006a). This statistic tests for departure from a constant-rate pure birth model. Negative γ values indicate a prevalence of nodes closer to the root than expected under a Pure Birth process, therefore suggesting a decreasing rate of diversification through time. Positive γ values indicate either an increasing rate or non-zero extinction rate (Pybus and Harvey 2000).

We compared the fit of the branching times to various models of lineage accumulation, using the Akaike Information Criterion (AIC), for the three semi-empirical datasets. AIC is calculated as $-2\iota + 2k$, where ι is the log-likelihood value and k is the number of free parameters of the model (Burnham and Anderson, 2002). All model- fitting analyses were conducted with the R packages LASER (Rabosky, 2006a) and TreePar (Stadler, 2011). The constant-rate models included PB (constant speciation rate λ and no extinction) and BD (constant speciation rate λ and extinction rate μ). Two density-dependent models were included, which assume that the diversification rate decreases as the lineage population reaches some threshold density. The density-dependent linear (DDL) model assumes that λ decreases linearly and there is no extinction. The density-dependent exponential (DDX) model assumes that λ decreases exponentially and there is no extinction (Rabosky and Lovette, 2008). λ and μ may also change through time in response to external factors. Therefore, we included Yule-2-rate (Rabosky, 2006b) and Birth-death-shift (BDS) (Stadler, 2011) models in order to test whether and when discrete shifts in diversification

rate occurred during the clade's history. In between shifts, these models simplify to the constant-rate PB or BD. The mean and SD of the –Log Likelihood value, models' parameters and AIC scores were computed for each of the semi-empirical datasets. In order to compare the relative fit of the models, the 95 % confidence interval of the AIC values was computed. The difference in AIC (dAIC) between each model and the best-fitting model (with the lowest AIC) was computed. Minimal and maximal dAIC were calculated considering the AIC values comprised in the 95 % confidence intervals. The amount of statistical confidence for each model is represented by the Akaike weights (wAIC).

In order to test rate-variable models that allow for increasing or decreasing rates of speciation, extinctions and declining diversity, we also used the method of (Morlon et al., 2011), implemented in the R package RPANDA. The fit of the following models was compared using the AIC: (1) Bcst: constant speciation rate, no extinction (PB); (2) Bvar: exponential variation of speciation rate, no extinction; (3) BvarDcst: exponential variation of speciation rate, constant extinction; (4) BcstDcst: constant speciation and extinction rates (BD); (5) BcstDvar : constant speciation and exponential variation in extinction rate; and (6) BvarDvar: exponential variation in both speciation and extinction rates. These models were tested assuming sampling fractions of 0.1, 0.5 and 0.72.

The BAMM (Bayesian Analysis of Macroevolutionary Mixtures) 2.4.0 (Rabosky, 2014) software was used to explore eventual shifts in regimes across the branches of a phylogenetic tree, a regime being a constant or time-varying process of speciation and extinction. These heterogeneous mixtures of macroevolutionary rate regimes are sampled with reversible-jump MCMC. Priors were estimated using the setBAMMpriors command. MCMC chains were run for 10 million generations, and sampled every thousand generations. We checked for convergence of the MCMC chains and ESS (at least more than 200) using the R package coda (Plummer et al., 2005). The first 10% of samples were discarded as burn-in. The R package BAMMtools (Rabosky et al., 2014) was used to calculate the BF and the 95% credibility set for the shift configurations and to plot diversification rates through time (Rabosky, 2014). BAMM analyses were computed assuming different levels of taxon sampling: 10, 50 and 72 %.

3. Results

3.1. Data overview

We obtained 132 COI, 139 28S and 159 H3 sequences of *Epimeria* species and related taxa, and three iphimediid sequences used as outgroup. The aligned COI sequences contained 613 bp, with 379 variable sites (among ingroup taxa). The 28S alignment was 1797 bp long (after removal of ambiguous regions with Aliscore), with 1154 variable sites. The length of the H3 alignment was 369 bp, with 119 variable sites. The datasets were concatenated, resulting in an alignment of 2779 bp. The best models and partitioning scheme suggested by PartitionFinder are indicated in Table 2. A single set of underlying branch lengths was assumed for the tree.

Subset Partitions	Best Model
28S	GTR + I + G
COI_pos1	SYM + I + G
COI_pos2	GTR + I + G
COI_pos3	GTR + I + G
H3_pos1, H3_pos2	JC + I
H3_pos3	GTR + G

Table 2. Best partitioning scheme and models of DNA substitution, inferred by PartitionFinder.

3.2. Phylogenetic analyses

Congruence between gene trees and methods – The ILD test rejected the null hypothesis of congruence between all tree comparisons (*p = 0.001*). Upon examination of the tree topologies, incongruences between the three gene trees affected mostly unsupported nodes. Only one supported phylogenetic relationship within the Papuasian clade of *Epimeria* sp. 3 differs between the COI and 28S gene trees. As this unique incongruence does not affect the conclusions of this study, the datasets were concatenated. Differences between the topologies of the two reconstruction methods (ML and BI) were minimal. In all cases, these ambiguities affected only unsupported nodes.

***Epimeria* and related taxa –** The Antarctic component of *Epimeria* is monophyletic with maximal support. All non-Antarctic *Epimeria* species also form a strongly supported clade (PP=1.00, BV=92). However, the monophyly of *Epimeria* is not supported by BI, as Antarctic *Epimeria* species form a sister clade to

two stilipedid species (PP=0.99), while this sister relationship remains unresolved by ML (BV=68). Deeper relationships between the Antarctic and non-Antarctic *Epimeria* clades, *Astyra abyssi*, the Acanthonotozomellid species and *Acanthonotozomopsis pushkini* are not supported. *Acanthonotozomoides oatesi* and *A. pushkini* form a maximally-supported clade (Fig. 1).

Antarctic *Epimeria* clade – The molecular systematics of the Antarctic *Epimeria* clade has been studied in detail in Verheye et al. (2016) and the morphological taxonomy in d'Udekem d'Acoz and Verheye (*in press*).

Non-Antarctic *Epimeria* clade – Twenty monophyletic morphospecies representing putatively new species are observed among Indo-Pacific *Epimeria* (Fig. 1). An indepth systematics study of these non-Antarctic *Epimeria* species is out of the scope of this paper and should be dealt with elsewhere.

Divergence times

The coefficients of variation were much higher than 0.1 for the three genes (COI: 1.1, 28S: 0.961, H3: 0.963), indicating that the sequences analyzed did not evolve at a constant rate along the branches. Therefore, we proceeded to use a relaxed molecular clock. Results of the path-sampling analysis and calculation of the BF are presented in Table 3. The UCED relaxed clock was strongly favored over the UCLD model. The BF strongly supports the Birth-Death over the Yule model (Table 3).

	MLE	2 lnBF
UCED	-36461	10278
UCLD	-41600	-
Birth-Death	-35922	34
Yule	-35939	-

Table 3. Marginal likelihood estimation (MLE) values recovered by path-sampling. Bayes Factors (2 lnBF) were estimated from the MLE to compare two relaxed clock models (UCED and UCLD) and two tree models (Yule and Birth-Death).

Bayesian posterior divergence times recovered by BEAST under an exponential relaxed clock model and Birth-Death tree model were consistent across the two runs. A mean age of 55.58 Ma (95 % HPD: 71.85–41.02 Ma) was estimated for the most recent common ancestor (MRCA) of the clade comprising the stilipedids and Antarctic *Epimeria*. The MRCA of the Antarctic *Epimeria* clade was given a mean age of 38.04 Ma (95 % HPD: 48.46–28.36 Ma). The MRCA of the non-Antarctic *Epimeria* clade was dated at 35.81 Ma (95 % HPD: 47.54–25.24 Ma), which separates into a Melanesian and an American-European-African lineage (Fig. 2).

3.3. Rates of diversification

Based on the γ statistic, we found no evidence of a decelerating lineage accumulation rate towards present time in the origination pattern of the Antarctic *Epimeria* clade. When incomplete sampling is taken into account, assuming 72 % or 50 % sampling, the γ values are positive, but the null hypothesis of constant rate of speciation is not rejected (*p>0.01*). When a 10 % sampling is assumed, the γ value is significantly positive (*p<0.01*), indicating either an increasing rate of speciation, or non-zero extinction (Table 4).

Dataset	γ	p-value 2-tailed
Semi-emp 10 %	11.02 (0.8)	0 (0)*
Semi-emp 50 %	1.419 (0.6)	0.14 (0.18)
Semi-emp 72 %	0.37 (0.47)	0.63 (0.21)
Empirical	-0.27	0.79

Table 4. Results of the CR test applied on the empirical and semi-empirical datasets.

No evident deviation from the null hypotheses of constant-rate models (BD or PB) is visible on the LTT plots (Fig. 3).

The BDL analyses indicate PB as the best supported model of lineage diversification, closely followed by Yule2rate.The estimated probability that PB is the best model for our data among the evaluated models (wAIC) is only 31 %, which demonstrates that the method does not strongly support one model over the others. Table 5 shows the results for the best-scoring models only and Table A1 for all models evaluated. When incomplete sampling is taken into

account, PB is the best model for the 72 % semi-empirical dataset (wAIC = 33 %), Yule2rate is the best model for the 50 % semi-empirical dataset (wAIC=27 %) and BD is the best model for the 10 % semi-empirical dataset (wAIC=62 %) (Table A1).

Models	LH	shift times	λ	AIC	dAIC	wAIC
PB	-28.47	-	0.078	58.94	0.00	0.31
Yule2rate	-26.62	2.09	0.088 0.027	59.24	0.30	0.27

Table 5. Parameter estimates and comparison of the fit of different lineage diversification models to the empirical dataset. Results are shown for the two best-scoring models. LH is the log-likelihood value of the model. The shift times (Ma) are indicated for the models implying discrete shifts in diversification rates. λ is the speciation rate. For each model, the Akaike Information criterion (AIC) was computed. The best-fitting model with the lowest AIC score is indicated in bold. dAIc is the difference between the AIC score of the evaluated model and the AIC score of the best-fitting model. wAIC are the Akaike weights.

The evaluation of Morlon et al.'s (2011) models of lineage diversification with RPANDA yielded the following results. When a 0.72 sampling fraction was assumed, Bcst (PB) was the best fit among the evaluated models (wAIC = 0.45), followed by Bvar (wAIC = 0.22), which implies an increasing speciation rate and no extinction. The Bvar model (again implying an increasing speciation rate and no extinction), was the best-fitting model when assuming a sampling fraction of 0.5. However, the latter had almost the same probability than Bcst (PB) of being the best fit among the evaluated models (wAIC = 0.32 and 0.30, respectively). For the 0.1 sampling fraction, Bvar (with an increasing speciation rate and no extinction) was also the best-fitting model with a wAIC of 0.54. Table 6 shows the results for the best-scoring models only and Table A2 for all models evaluated.

Dataset	Model	AIC	dAIC	wAIC	λ	α
Sampling 72 %	Bcst	243.44	0.00	0.45	0.093	-
	Bvar	244.88	1.44	0.22	0.11	-0.015

Sampling 50 %	Bcst	244.34	0.16	0.30	0.11	-
	Bvar	244.18	0.00	0.32	0.14	-0.03
Sampling 10 %	Bvar	242.72	0.00	0.54	0.37	-0.07

Table 6. Parameter estimates and comparison of the fit of Morlon et al.'s (2011) lineage diversification models with RPANDA. Results are shown for the best-scoring model and the second best fit whenever the wAIC of the best-scoring model was < 0.5. For each model, the Akaike Information criterion (AIC) was computed. The best-fitting model with the lowest AIC score is indicated in shaded grey. dAIC is the difference between the AIC score of the evaluated model and the AIC score of the best-fitting model. wAIC are the Akaike weights. λ is the speciation rate and α is the parameter controlling the exponential variation of the speciation rate with time.

For all considered sampling fractions (0.72, 0.5 and 0.1), the maximum posterior probability (MAP) shift configuration returned by BAMM — which is the distinct shift configuration with the highest posterior probability— is a single macroevolutionary regime across the whole tree and, i.e. no discrete rate shift. This is also the only regime contained in the 95 % credible shift set. Bayes Factor analyses also favour a model with no rate shifts, for all sampling scheme (Table 7). The rate through time plots show a constant diversification rate for the 0.72 sampling scheme, while it is increasing for the 0.1 and 0.5 sampling schemes (Fig. 4). However, the current version of BAMM assumes that all regimes are time-variable. In order to investigate the rate variation observed for the 0.1 and 0.5 sampling schemes, we computed the 95 % Higher Posterior Density (HPD) interval of the post-burnin samples of the lambda shift parameter. This parameter is the standard deviation of the normal distribution of speciation rates. A value of zero therefore indicates rate constancy. As the 95 % HPD of the lambda shift parameter includes 0 in both cases (95 % HPD for 10 % sampling [-0.005, 0.057] and for 50 % sampling [-0.022; 0.057]), there is no evidence for a variable speciation rate.

	Sampling	**1 shift**	**2 shifts**	**3 shifts**
0 shift	**10 %**	21.522	137.203	-
	50 %	9.729	60.878	213.075
	72 %	7.495	32.676	95.057

Table 7. Matrix of pairwise Bayes Factors (BF), where the BF is the ratio of marginal likelihoods between two models, Mi and Mj. Numerator models are given as rows and denominator models as columns. BF > 3 is considered positive support for Mi, while > 20 is a strong support (Kass and Raftery, 1995).

4. Discussion

4.1. Systematics of *Epimeria*

The monophyly of *Epimeria* was not supported by BI, as two species of Stilipedidae from the subfamily Alexandrellinae (*Bathypanoploea schellenbergi* and *Alexandrella dentata*) are sister to the Antarctic *Epimeria* clade (PP=0.99). The systematics of *Epimeria* should therefore be revised, as the genus may potentially include (at least part of) the Stilipedidae. This latter family was divided into three subfamilies: Astyrinae, Stilipedinae and Alexandrellinae (Holman and Watling, 1983). However, Stilipedidae is not monophyletic, as *Astyra abyssi* (from the subfamily Astyrinae) is not sister to Alexandrellinae neither in the present study nor in a previous phylogeny of Eusiroidea (Verheye et al. 2015). Since the systematics of Stilipedidae remains unclear, we will consider here only the Alexandrellinae as a potential sister clade to the Antarctic *Epimeria*. However, as this relationship is supported by low BV (68) and PP values have been shown to lead to higher type I error rates (Erixon et al., 2003), the support of this node should be verified with additional data before making any taxonomic changes. The main differences between *Epimeria* and *Alexandrella* reside in the mouthpart morphology. Several possible autapomorphies indeed characterize the *Alexandrella*: (1) the mandibular molar is absent, (2) the palp of the maxilla 1 is expanded, (3) the inner and outer plates of the maxilla 2 are expanded and (4) the outer plate of the maxilliped is greatly expanded (Holman and Watling, 1983). Moreover, the non-ommatidian eyes in Alexandrellinae could be indicative of a deep-sea ancestor (Warrant and Locket, 2004). If the Alexandrellinae are indeed nested within *Epimeria*, a shift of trophic niche and/or bathymetric range of their ancestor could have led to these morphological modifications.

4.2. Isolation of Antarctic *Epimeria* or historical dispersals?

As Antarctic *Epimeria* species are monophyletic and the origin of this Antarctic clade is estimated to be older or contemporaneous to the geographical isolation of Antarctica, it is hypothesized that *Epimeria* did not disperse in/out of the shelf throughout its evolutionary history. However, to further test the monophyly of this Antarctic component, it would be interesting to include the single Magellanic (*Metepimeria acanthurus*) and sub-Antarctic (*Epimeria ashleyi,* from the Macquarie Ridge) *Epimeria* species in the phylogenetic tree.

The Antarctic shelf is well isolated from the other ocean's shelves by large distances (> 850 km), deep seas and the most powerful current on earth, the ACC (Clarke et al., 2005; Orsi et al., 2005). Moreover, beyond the APF, surface water temperatures rise by 3–4 °C. Because of their limited tolerance to such temperature change, many Antarctic marine invertebrates would not be able to establish on the other side of the APF (Peck, 2002). *Epimeria* is presumably cold-adapted, as outside the Antarctic region, it is mainly found at bathyal depths. Temperature is therefore likely to be an important isolating factor for the Antarctic *Epimeria* clade. However, historical movements of stenothermal taxa in and out of the Antarctic shelf could have been possible during periods of climatic changes (Clarke et al., 1992). A variety of pelagic organisms (or organisms with a pelagic life stage) were reported to cross the APF, supposedly by means of eddies, i.e. water masses transported out of the ACC (Antezana, 1999; Clarke et al., 2005; Li et al., 2002) or by the Antarctic Intermediate water that extends northwards (Antezana, 1999). As such currents do not reach the ocean floor (Clarke et al., 2005), benthic taxa lacking a pelagic larval stage can only disperse through the deep-sea. Historical events of such polar emergences (i.e. colonization of the shelf by deep-sea fauna) and submergences (i.e. colonization of the deep-sea by shelf fauna) did occur in the evolutionary history of some strictly benthic taxa (Held, 2000; Raupach et al., 2007; Strugnell et al., 2008, 2011). Such movement is indeed facilitated by the thermohaline circulation, which connects the Southern Ocean shelf with the deep waters of the other world's oceans through an isothermal water column, and by the unusually deep Antarctic shelf (reaching > 1000 m at places) (Clarke, 2003; Clarke et al., 2009; Rogers, 2000). Polar submergences occurred in the Antarctic *Epimeria* clade history: whereas the vast majority of Antarctic *Epimeria* species are found on the shelf and upper slope (< 1200 m), two species (*Epimeria larsi* and *Epimeria* sp. 2) nested within shelf clades have bathymetric distributions restricted to slope depths (around 2000 m). However, the Drake Passage has an average depth of 3400 m (Smith and Sandwell, 1997). The bathymetric distributions of *Epimeria* species worldwide suggest that this might be too deep for most *Epimeria* to disperse in and/or out of the Antarctic region along the benthos, which would explain the evolutionary isolation of the Antarctic clade. However, two species were sampled in the abyssal plain: *Epimeria glaucosa* was found at 3710 m around New Zealand (Barnard, 1961) and *Epimeria abyssalis* at around 5600 m in the Kuril-Kamchatka Trench (Shimomura and Tomikawa, 2016). Additional deep-sea sampling and inclusion of abyssal species in phylogenetic analyses might reveal undetected historical dispersal of *Epimeria* through the deep-sea.

4.3 Origin and historical biogeography of Antarctic *Epimeria*

The first hypothesis aiming at determining the temporal and geographical origin of Antarctic *Epimeria* was presented by Lörz and Held (2004). Ages of between 34.9 and 15.7 Ma were inferred for the MRCA of *Epimeria*, based on COI distances and rates estimated for cirripeds (3.1 %/Myr) and for alpheid shrimps (2.4 %/Myr), and assuming a strict molecular clock. Applying a relaxed clock model on a combined dataset (COI, 28S and H3), we obtained a mean COI rate estimate of 1.6 %/Myr and an age of 38.04 Ma (95% HPD [48.46 Ma; 28.36 Ma]) for the MRCA of the Antarctic *Epimeria* clade. As the 95 % HPD interval spans an older period than the age estimation of Lörz and Held (2004), the assumption that this clade originated when Antarctica was already isolated from the other fragments of Gondwana is equivocal (Figure 2).

From the Late Cretaceous to the early Cenozoic, Antarctica, South America, Australia and New Zealand were connected in an area of cool temperate shallow seas known as the Weddelian Province (Woodburne and Zinsmeister, 1984; Zinsmeister, 1979, 1984). The South Tasman Saddle, a submarine trough between Tasmania and the South Tasman Rise, existed as a shallow to medium-depth seaway in the late Paleocene to early Eocene. If the Antarctic George V and Oates Coast shelf breaks were closer to the present shoreline at that time, it is possible that a deep seaway between Australia and East Antarctica existed as early as 40 Ma. Otherwise, a deepwater passage only developed after the late Eocene (Lawver et al., 2013, 2014). It has indeed been inferred that the Tasmanian gateway deepened in the period 35.5 to 30.2 Ma (Stickley et al., 2004) and was open to unrestricted deepwater circulation at 32 Ma (Lawver and Gahagan, 2003). An early opening of the Drake Passage to shallow water was suggested to have taken place in the Middle to Late Eocene (50–41 Ma) (Eagles et al., 2006; Livermore et al., 2005; Scher and Martin, 2004). This was followed by a progressive widening and deepening to intermediate depth at 37 Ma, while the deepwater passage is usually dated in the interval 34–30 Ma (Lagabrielle et al., 2009; Latimer and Filippelli, 2002; Lawver and Gahagan, 2003; Livermore et al., 2005; Scher and Martin, 2004) (Figure 2). The opening of the Tasmanian and Drake passages were inferred as important vicariant events, promoting speciation in other Antarctic benthic shelf species (Göbbeler and Klussmann-Kolb, 2010; Lee et al., 2004; Matschiner et al., 2011; Near, 2004).

It cannot be inferred from the current data whether the Antarctic *Epimeria* clade originated in the Weddelian Province or by vicariance when the continent separated from the other Gondwanan fragments. The divergence from its stilipedid sister clade (*Bathypanoploea schellenbergi* and *Alexandrella dentata*) occurred 55.58 Ma (95 % HPD [71.85; 41.02 Ma]), in the Weddelian Province (Figure 2). However, the inclusion of additional non-Antarctic samples — especially from historically connected and geographically closer regions such as South America, Australia and the sub-Antarctic islands — may help to

identify the sister lineage of the Antarctic *Epimeria* clade and shed light on its biogeographic origin. The endemicity of the Antarctic *Epimeria* clade would suggest that it originated *in situ* when the region was already isolated. In the case that this isolation was not yet geographical, it was suggested that a latitudinal gradient in seasonality might have promoted an early Cenozoic divergence of the polar fauna (Crame, 2013).

In any way, the initial diversification of the Antarctic *Epimeria* lineage would have occurred in a cooling environment. Following the early Eocene Climatic Optimum (EECO), high latitude surface water began to cool across the early to middle Eocene boundary (49–48 Ma) (Lawver and Gahagan 2003). A second cooling phase occurred in the late Middle Eocene 44–41 Ma. From the beginning of this cooling trend, the ice sheets progressively grew to culminate at the Eocene–Oligocene boundary (Miller et al., 2008). The transition to an icehouse climate in the earliest Oligocene, known as the Eocene-Oligocene Climate Transition (EOCT), was marked by an abrupt cooling at 33.55 Ma (Miller et al., 1991) and the first continent-wide glaciations (Hambrey et al., 1991; Sorlien et al., 2007; Wilson et al., 2013). Most of the species complexes identified in Verheye et al. (2016) diversified after the MMCT, (~14 Ma), a period marking the beginning of repeated ice sheet advances over the shelf and retreats inshore (Shevenell et al., 2004). Globally, these results suggest that the Antarctic *Epimeria* clade's diversification would be related to cold waters (Figure 2). Many modern Antarctic lineages likely arose in the time period spanning this transition from Eocene cool-temperate climate to Oligocene polar climate, as the fossil record indicates a fundamental shift in the structure of benthic communities. The extinction of many durophagous (skeleton-crushing) predator taxa — decapods, teleost and cartilaginous fishes — decreased the predation pressure, which allowed the establishment of dense populations of erect sessile suspension feeders (Aronson et al., 2007). These organisms constitute a food source for many amphipods, which are predatory food specialists (e.g. Coleman, 1989, 1991; Klages and Gutt, 1990). Moreover, sessile suspension-feeders form dense assemblages which provide a three-dimensionally structured habitat for an errant fauna of mostly slow-moving invertebrates, such as amphipods (Arntz et al., 2005; Aronson and Blake, 2001; Clarke et al., 2004; Clarke and Crame, 2010). In summary, the adaptation of *Epimeria* to a cold environment, coupled with the extinction of cold-intolerant taxa and resulting abundant available niche-space likely led to their successful diversification on the Antarctic shelf.

The divergence between a clade entirely composed of Melanesian species and a clade that includes European, African and South-American species occurred 35.81 Ma 95% HPD [47.54 Ma; 25.24 Ma] (Figure 2). The Indo-Pacific islands were likely not colonized by *Epimeria* species from the Weddelian Province or

Australia, but rather from south-eastern continental Asia. Indeed, at the time of origin of this Melanesian clade, the South East Asian gateway that connects the Indian and Pacific oceans was widely opened, likely forming an efficient barrier to dispersion between Australia and the Indo-Pacific region (Hall et al., 2011).

4.4 Diversification of *Epimeria* on the Antarctic shelf

No early diversification burst was detected in the phylogenetic pattern of the Antarctic *Epimeria* clade, nor any shift in diversification rates associated with glacial cycles. The Antarctic *Epimeria* clade has survived through multiple mass extinction events associated with the cooling of the continent and the glacial cycles. The fossil record indeed indicates many biotic turnovers induced by climate change (Beu, 2009; Crame et al., 2014; Hara, 2001). Furthermore, it was shown that following the MMCT, the ice sheet extended to the outer shelf during glacial maxima, at least in some places, thereby erasing shelf habitats and their associated biota (e.g. Chow and Bart, 2003; Hambrey and McKelvey, 2000; Passchier et al., 2003).

Despite the evidence for repeated extinctions of the Antarctic shelf biota, the extinction rate estimates given by the different methods used herein are unrealistically close to zero. Extinction rate estimates from phylogenies of extant taxa were often shown to be unreliable (Nee, 2006; Purvis, 2008; Rabosky, 2010; Rabosky and Lovette, 2008; Ricklefs, 2007). In the present case, the phylogeny may simply lack sufficient information to accurately estimate extinction rates or infer diversity dynamics (Liow et al., 2010; Morlon et al., 2011; Quental and Marshall, 2009; Rabosky, 2010).

Mass extinctions are believed to promote adaptive radiations, manifested by a subsequent sharp increase in the rate of diversification (Benton and Emerson, 2007; Condamine et al., 2013; McInnes et al., 2011). These “rebounds” would be followed by a density-dependent decrease in diversification rates. However, if repeated mass extinctions occurred, the signals of older pulses of diversification tend to be eroded by subsequent extinctions (Phillimore and Price, 2008; Rabosky and Lovette, 2008; Ricklefs and Jønsson, 2014; Weir, 2006). Because of the presumed high turnover rate in the evolutionary history of the Antarctic *Epimeria* clade, even a large early diversification burst could be undetectable (McInnes et al., 2011; Quental and Marshall, 2009; Rabosky and Lovette, 2008). However, without a fossil record, we cannot determine whether this turnover rate was sufficiently high compared to the initial speciation rate to erode an early burst signature (Quental and Marshall, 2009).

If the history of environmental disturbances is responsible for the lack of an early burst signature, then we can expect similar patterns in other benthic shelf taxa. The paucity of branching events between the Oligocene and MMCT in the notothenioid fishes' phylogeny was interpreted as unobserved extinction, possibly eroding the signature of an explosive early radiation. However, the latter study also provided evidence of evolutionary radiations for several younger subclades, coinciding with the MMCT climate change event (Near et al., 2012).

The relatively low number of tips in our phylogeny might decrease the statistical power of the tests to detect lineage-specific shifts. It has been shown that a reduced taxon sampling compromises the detection of discrete rate shifts and slowdowns in diversification (Laurent et al., 2015; Phillimore and Price, 2008, 2009). This could also explain the inability of the model-selection analyses to discriminate between different equally fitting models. When the true diversity of the clade is better known, diversification analyses repeated on a thoroughly sampled phylogeny might reveal unobserved diversification regime changes.

Finally, in order to detect an early burst of diversification, the clade must also be close to its equilibrium diversity (McInnes et al., 2011; Quental and Marshall, 2010). Yet, the Antarctic *Epimeria* clade may still be in the earliest stage of a logistic growth following the Last Glacial Maximum. The exponential growth of diversity that would be observed in such case (Liow et al., 2010; Quental and Marshall, 2010) is consistent with our results of either constant or increasing rates of speciation. Assuming that the dynamics of the Antarctic *Epimeria* clade is governed by diversity-dependent diversification, there is, however, no way of determining in which stage of its diversification trajectory this clade actually stands (Quental and Marshall, 2010).

5. Conclusions

By including species from all the world's oceans and by applying a relaxed clock model to date the phylogeny, this study provides the first spatiotemporal framework for the evolution of Antarctic *Epimeria*. Although the precise timing of origin of the Antarctic clade is still debatable, our data suggest that this lineage originated *in situ* — in the Late Gondwanan Weddellian Province or by vicariance when the plates broke apart — and does not result from a colonization event after the geographical isolation of the continent. The initial diversification of the clade occurred in a cooling environment, which suggests that the adaptation of this genus to cold waters, along with the extinction of cold-intolerant taxa and resulting availability of habitats, would have led to their successful radiation on the Antarctic shelf. The Antarctic *Epimeria* clade appears to have evolved in complete isolation from the other world's oceans,

as our data do not provide any evidence of dispersal in and/or out of the shelf since the isolation of Antarctica. Sampling of additional non-Antarctic *Epimeria*, especially from historically connected regions (South America, Australia and New Zealand), could help identify the sister lineage of the Antarctic clade and clarify its biogeographical origin.

Acknowledgements

This work was supported by a Ph.D. fellowship from F.R.I.A. (F.N.R.S., Belgium). The last author was funded by the Digit 3 program of BELSPO. We thank the Alfred-Wegener-Institut, Helmholtz-Zentrumfür Polar- und Meeresforschung (AWI) and the captain, crew and chief scientists of various R.V. Polarstern expeditions for their efficiency, as well as present and past colleagues of the staff of the Royal Belgian Institute of Natural Sciences (RBINS), especially Henri Robert and Charlotte Havermans, for collecting specimens on board. The travel expenses of the first and last authors during ANT-XXIX/3 were funded by the Fonds Léopold III. The research program led by Guillaume Lecointre, REVOLTA 1124, supported by the Institut polaire français Paul Emile Victor (IPEV) and the Muséum national d'Histoire naturelle (MNHN), and the CAML-CEAMARC cruise of RSV Aurora Australis (IPY project no. 53), supported by the Australian Antarctic Division, the Japanese Science Foundation and the IPEV (project ICOTA), are acknowledged for providing extensive Antarctic material. The Melanesian specimens used in this study were collected during various deep-sea cruises, conducted respectively by MNHN and Institut de Recherche pour le Développement (IRD) as part of the Tropical Deep-Sea Benthos programme (http://expeditions.mnhn.fr/program/tropicaldeep-seabenthos). Funders and sponsors include the French Ministry of Foreign Affairs, the Total Foundation, Prince Albert II of Monaco Foundation, Stavros Niarchos Foundation, and Richard Lounsbery Foundation. We thank Laure Corbari (MNHN) for giving us access to this material. This publication is registered as CAML (Census of Antarctic Marine Life) publication No. 164 and contribution No. 215 to ANDEEP. We are also grateful to Zohra Elouaazizi (RBINS), Karin Breugelmans (RBINS) and Gontran Sonet (RBINS- JEMU) for helpful methodological advices. TB contributed to this manuscript on behalf of the "Joint Experimental Molecular Unit" (RBINS-JEMU) and the FWO Research Community W0.009.11N "Belgian Network for DNA Barcoding" (BeBoL).

References

Angel, M.V., 1997. Pelagic biodiversity. In: Ormond, R.F.G.*e.a.* (Ed.), Marine biodiversity: causes and consequences. Cambridge University Press, pp. 35-68.

Antezana, T., 1999. Plankton of Southern Chilean fjords: trends and linkages. Scientia Marina 63, 69-80.
Arntz, W., Gutt, J., Klages, M., 1997. Antarctic marine biodiversity: an overview. In: B. Battaglia, J.V., D. Walton (Ed.), Antarctic communities: proceedings of the 6th SCAR Biology Symposium. Cambridge University Press, Venice.
Arntz, W.E., Thatje, S., Gerdes, D., Gili, J.M., Gutt, J., Jacob, U., Montiel, A., Orejas, C., Teixido, N., 2005. The Antarctic-Magellan connection: macrobenthos ecology on the shelf and upper slope, a progress report. Scientia Marina 69, 237-269.
Aronson, R.B., Blake, D.B., 2001. Global climate change and the origin of modern benthic communities in Antarctica. American Zoologist 41, 27-39.
Aronson, R.B., Thatje, S., Clarke, A., Peck, L.S., Blake, D.B., Wilga, C.D., Seibel, B.A., 2007. Climate Change and Invasibility of the Antarctic Benthos. Annual Review of Ecology, Evolution, and Systematics 38, 129-154.
Barber, H.N., Dadswell, H.E., Ingle, H.D., 1959. Transport of Driftwood from South America to Tasmania and Macquarie Island. Nature 184, 203-204.
Bargelloni, L., Marcato, S., Zane, L., Patarnello, T., 2000. Mitochondrial phylogeny of notothenioids: a molecular approach to Antarctic fish evolution and biogeography. Systematic Biology 49, 114-129.
Barker, P.F., 2001. Scotia Sea regional tectonic evolution: implications for mantle flow and palaeocirculation. Earth-Science Reviews 55, 1-39.
Benton, M.J., Emerson, B.C., 2007. How did life become so diverse? The dynamics of diversification according to the fossil record and molecular phylogenetics. Palaeontology 50, 23-40.
Beu, A.G., 2009. Before the ice: Biogeography of Antarctic Paleogene molluscan faunas. Palaeogeography, Palaeoclimatology, Palaeoecology 284, 191-226.
Bouckaert, R., Drummond, A., 2015. bModelTest: Bayesian phylogenetic site model averaging and model comparison. BMC Evolutionary Biology 17, 42.
Bouckaert, R., Heled, J., Kuhnert, D., Vaughan, T., Wu, C.H., Xie, D., Suchard, M.A., Rambaut, A., Drummond, A.J., 2014. BEAST 2: a software platform for Bayesian evolutionary analysis. PLoS Comput Biol 10, e1003537.
Brandt, A., 1992. Origin of Antarctic Isopoda (Crustacea, Malacostraca). Mar Biol 113, 415-423.
Brandt, A., 1999. On the origin and evolution of Antarctic Peracarida (Crustacea, Malacostraca). Scientia Marina 63, 261-274.
Brandt, A., Gooday, A.J., Brandao, S.N., Brix, S., Brokeland, W., Cedhagen, T., Choudhury, M., Cornelius, N., Danis, B., De Mesel, I., Diaz, R.J., Gillan, D.C., Ebbe, B., Howe, J.A., Janussen, D., Kaiser, S., Linse, K., Malyutina, M., Pawlowski, J., Raupach, M., Vanreusel, A., 2007. First insights into the biodiversity and biogeography of the Southern Ocean deep sea. Nature 447, 307-311.
Briggs, D.E., Kear, A.J., 1994. Decay and Mineralization of Shrimps. Palaios 9, 431.
Briggs, D.E., Wilby, P.R., 1996. The role of the calcium carbonate-calcium phosphate switch in the mineralization of soft-bodied fossils. Journal of the geological Society 153, 665-668.
Burnham, K.P., Anderson, D.R., 2002. Model selection and multimodel inference: a practical information theroretical approach, second edition. Springer-Verlag, New York, USA.
Chow, J.M., Bart, P.J., 2003. West Antarctic Ice Sheet grounding events on the Ross Sea outer continental shelf during the middle Miocene. Palaeogeography, Palaeoclimatology, Palaeoecology 198, 169-186.
Clarke, A., 2003. Costs and consequences of evolutionary temperature adaptation. Trends in Ecology & Evolution 18, 573-581.
Clarke, A., Aronson, R.B., Crame, J.A., Gili, J.M., Blake, D.B., 2004. Evolution and diversity of the benthic fauna of the Southern Ocean continental shelf. Antarctic Science 16, 559-568.

Clarke, A., Barnes, D.K., Hodgson, D.A., 2005. How isolated is Antarctica? Trends in Ecology & Evolution 20, 1-3.
Clarke, A., Crame, J.A., 1989. The origin of the Southern Ocean marine fauna. In: Crame, J.A. (Ed.), Origin and evolution of the Antarctic biota. Geological Society of London Special Publication, London, pp. 253-268.
Clarke, A., Crame, J.A., 1997. Diversity, latitude and time: patterns in the shallow sea. In: Ormond, R.F.G., Gage, J.D., Angel, M.V. (Ed.), Marine Biodiversity: patterns and processes. Cambridge University Press, Cambridge, pp. 122-147.
Clarke, A., Crame, J.A., 2010. Evolutionary dynamics at high latitudes: speciation and extinction in polar marine faunas. Philosophical Transactions of the Royal Society B: Biological Sciences 365, 3655-3666.
Clarke, A., Crame, J.A., Stromberg, J.O., Barker, P.F., 1992. The Southern Ocean Benthic Fauna and Climate Change: A Historical Perspective [and Discussion]. Philosophical Transactions: Biological Sciences 338, 299-309.
Clarke, A., Griffiths, H.J., Barnes, D.K.A., Meredith, M.P., Grant, S.M., 2009. Spatial variation in seabed temperatures in the Southern Ocean: implications for benthic ecology and biogeography. Journal of Geophysical Research: Biogeosciences 114, 1-11.
Clarke, A., Johnston, I.A., 1996. Evolution and adaptive radiation of Antarctic fishes. Trends in Ecology & Evolution 11, 212-218.
Clarke, A., Johnston, N.M., 2003. Antarctic marine benthic diversity. In: Atkinson, R.N.G.R.J.A. (Ed.), Oceanography and marine biology: an annual review. Taylor & Francis, London, pp. 47-114.
Coleman, C.O., 1989. On the nutrition of two Antarctic Acanthonotozomatidae (Crustacea: Amphipoda). Polar Biology 9, 287-294.
Coleman, C.O., 1991. Comparative fore-gut morphology of Antarctic Amphipoda (Crustacea) adapted to different food sources. Hydrobiologia 223, 1-9.
Coleman, C.O., 2004. Aquatic amphipods (Crustacea: Amphipoda: Crangonyctidae) in three pieces of Baltic amber. Organisms Diversity & Evolution Electr. Suppl. 3, 1-7.
Coleman, C.O., Myers, A.A., 2000. New Amphipoda from Baltic amber. Polskie Archiwum Hydrobiologii 47, 457-464.
Coleman, C.O., Ruffo, S., 2002. Another discovery of a niphargid amphipod (Crustacea) in Baltic amber. Geol.-Paläontol. Inst. Univ. Hamburg 86, 239-244.
Coleman, O.C., 2007. Synopsis of the Amphipoda of the Southern Ocean. Bulletin de l'Institut Royal des Sciences Naturelles de Belgique 77 Suppl.2, 1-134.
Colgan, D., McLauchlan, A., Wilson, G., Livingston, S., Edgecombe, G., 1998. Histone H3 and U2 snRNA DNA sequences and arthropod molecular evolution. Australian Journal of Zoology 46, 419-437.
Condamine, F.L., Rolland, J., Morlon, H., 2013. Macroevolutionary perspectives to environmental change. Ecology Letters 16, 72-85.
Coombs, D.S., Landis, C.A., 1966. Pumice from the South Sandwich Eruption of March 1962 reaches New Zealand. Nature 209, 289-290.
Costa, A., 1851. Fauna del Regno di Napoli (and) Catalogo de' Crostacei del Regno di Napoli. Catalogo dei Crostacei Italiani e di Molti Altri del Mediterraneo per Fr. Gugl. Hope. F. Azzolino, Napoli, pp. 1-48.
Crame, J.A., 2013. Early Cenozoic Differentiation of Polar Marine Faunas. PloS one 8, e54139.
Crame, J.A., Beu, A.G., Ineson, J.R., Francis, J.E., Whittle, R.J., Bowman, V.C., 2014. The Early Origin of the Antarctic Marine Fauna and Its Evolutionary Implications. PloS one 9, e114743.
Cusimano, N., Stadler, T., Renner, S.S., 2012. A new method for handling missing species in diversification analysis applicable to randomly or nonrandomly sampled phylogenies. Systematic Biology 61, 785-792.

De Broyer, C., Jażdżewska, A., 2014. Chapter 5.17. Biogeographic patterns of Southern Ocean benthic Amphipods. In: De Broyer C, K.P., Grifftiths H, Raymond B, d'Udekem d'Acoz C (Ed.), Biogeographic Atlas of the Southern Ocean. Committee on Antarctic Research, Cambridge.
Dell, R.K., 1972. Antarctic benthos. Advanced Marine Biology 10, 1-216.
Drummond, A.J., Bouckaert, R.R., 2015. Bayesian evolutionary analysis wit BEAST. Cambridge University Press, Cambridge.
Eagles, G., Livermore, R., Morris, P., 2006. Small basins in the Scotia Sea: the Eocene Drake Passage gateway. Earth and Planetary Science Letters 242, 343-353.
Erixon, P., Svennblad, B., Britton, T., Oxelman, B., 2003. Reliability of Bayesian posterior probabilities and bootstrap frequencies in phylogenetics. Syst Biol 52, 665-673.
Exon, N., Kennett, J., Malone, M., Brinkhuis, H., Chaproniere, G., Ennyu, A., Fothergill, P., Fuller, M., Grauert, M., Hill, P., Janecek, T., Kelly, C., Latimer, J., McGonigal, K., Nees, S., Ninnemann, U., Nuernberg, D., Pekar, S., Pellaton, C., Pfuhl, H., Robert, C., Röhl, U., Schellenberg, S., Shevenell, A., Stickley, C., Suzuki, N., Touchard, Y., Wei, W., White, T., 2000. The opening of the Tasmanian Gateway drove global Cenozoic paleoclimatic and paleoceanographic changes; results of Leg 189. Affiliation (analytic): Australian Geological Survey Organisation, Canberra, A.C.T. 26, 11.
Farris, J.S., Källersjö, M., Kluge, A.G., Bult, C., 1995. Testing significance of incongruence. Cladistics 10, 315-319.
Fraser, C.I., Nikula, R., Spencer, H.G., Waters, J.M., 2009. Kelp genes reveal effects of subantarctic sea ice during the Last Glacial Maximum. Proceedings of the National Academy of Sciences 106, 3249-3253.
Freckleton, R.P., Harvey, P.H., 2006. Detecting non-Brownian trait evolution in adaptive radiations. PLoS Biol 4, e373.
Göbbeler, K., Klussmann-Kolb, A., 2010. Out of Antarctica? New insights into the phylogeny and biogeography of the Pleurobranchomorpha (Mollusca, Gastropoda). Molecular Phylogenetics and Evolution 55, 996-1007.
Hall, R., Cottam, M.A., Wilson, M.E.J., 2011. The SE Asian gateway: history and tectonics of the Australia–Asia collision. Geological Society, London, Special Publications 355, 1-6.
Hambrey, M.J., Ehrmann, W.U., Larsen, B., 1991. Cenozoic glacial record of the Prydz Bay continental shelf, East Antarctica. Affiliati 119, 77.
Hambrey, M.J., McKelvey, B., 2000. Major Neogene fluctuations of the East Antarctic ice sheet: stratigraphic evidence from the Lambert Glacier region. Geology 28, 887-890.
Hara, U., 2001. Bryozoans from the Eocene of Seymour Island Antarctic Peninsula. In: Gazdzicki, A. (Ed.), Palaeontological results of the polish Antarctic expeditions. Part III. Paleontologia Polonica, Poland, pp. 33-156.
Held, C., 2000. Phylogeny and biogeography of serolid isopods (Crustacea, Isopoda, Serolidae) and the use of ribosomal expansion segments in molecular systematics. Molecular Phylogenetics and Evolution 15, 165-178.
Helmuth, B., Veit, R.R., Holberton, R., 1994. Long-distance dispersal of a subantarctic brooding bivalve (*Gaimardia trapesina*) by kelp-rafting. Mar Biol 120, 421-426.
Ho, S.Y.W., Saarma, U., Barnett, R., Haile, J., Shapiro, B., 2008. The effect of inappropriate calibration: three case studies in molecular ecology. PloS one 3, e1615.
Hodgson, D., Vyverman, W., Peters, T.A., 1997. Diatoms of meromictic lakes adjacent to the Gordon River, and of the Gordon River estuary in south-west Tasmania. Bibliotheca Diatomologica 35, 1-172.
Holman, H., Watling, L., 1983. A revision of the Stilipedidae (Amphipoda). Crustaceana 44, 27-53.

Hou, Z., Fu, J., Li, S., 2007. A molecular phylogeny of the genus *Gammarus* (Crustacea: Amphipoda) based on mitochondrial and nuclear gene sequences. Molecular Phylogenetics and Evolution 45, 596-611.
Hunter, R.L., Halanych, K.M., 2008. Evaluating connectivity in the brooding brittle star *Astrotoma agassizii* across the Drake Passage in the Southern Ocean. Journal of Heredity 99, 137-148.
Jażdżewski, K., Kulicka, R., 2000b. A note on amphipod crustaceans in a piece of Baltic amber. Annals of Zoology 50, 99-100.
Kass, R.E., Raftery, A.E., 1995. Bayes factors. Journal of the American Statistical Association 90, 773-795.
Katoh, K., Standley, D.M., 2013. MAFFT multiple sequence alignment software version 7: improvements in performance and usability. Molecular Biology and Evolution 30, 772-780.
Klages, M., Gutt, J., 1990. Comparative studies on the feeding behaviour of high Antarctic amphipods (Crustacea) in laboratory. Polar Biology 11, 73-79.
Klaus, S., Schubart, C.D., Streit, B., Pfenninger, M., 2010. When Indian crabs were not yet Asian--biogeographic evidence for Eocene proximity of India and Southeast Asia. BMC Evolutionary Biology 10, 287.
Knox, G.A., Lowry, J.K., 1977. A comparison between the benthos of the Southern Ocean and the North Polar Ocean with special reference to the Amphipoda and Polychaeta. In: Dunbar, M.J. (Ed.), Polar oceans Proceedings of the Polar Ocean Conference, Calgary, pp. 432-462.
Lagabrielle, Y., Goddéris, Y., Donnadieu, Y., Malavieille, J., Suarez, M., 2009. The tectonic history of Drake Passage and its possible impacts on global climate. Earth and Planetary Science Letters 279, 197-211.
Lanfear, R., Calcott, B., Ho, S.Y., Guindon, S., 2012. Partitionfinder: combined selection of partitioning schemes and substitution models for phylogenetic analyses. Molecular Biology and Evolution 29, 1695-1701.
Lartillot, N., Philippe, H., 2006. Computing Bayes factors using thermodynamic integration. Systematic Biology 55, 195-207.
Latimer, J.C., Filippelli, G.M., 2002. Eocene to Miocene terrigenous inputs and export production: geochemical evidence from ODP Leg 177, Site 1090. Palaeogeography, Palaeoclimatology, Palaeoecology 182, 151-164.
Laurent, S., Robinson-Rechavi, M., Salamin, N., 2015. Detecting patterns of species diversification in the presence of both rate shifts and mass extinctions. BMC Evolutionary Biology 15, 15-157.
Lawver, L.A., Gahagan, L.M., 2003. Evolution of Cenozoic seaways in the circum-Antarctic region. Palaeogeography, Palaeoclimatology, Palaeoecology 198, 11-37.
Lear, C.H., Elderfield, H., Wilson, P.A., 2000. Cenozoic deep-sea temperatures and global ice volumes from Mg/Ca in benthic foraminiferal calcite. Science 287, 269-272.
Lear, C.H., Rosenthal, Y., Coxall, H.K., Wilson, P., 2004. Late Eocene to early Miocene ice sheet dynamics and the global carbon cycle. Paleoceanography 19.
Lecointre, G., Ameziane, N., Boisselier, M.C., Bonillo, C., Busson, F., Causse, R., Chenuil, A., Couloux, A., Coutanceau, J.P., Cruaud, C., d'Acoz, C., De Ridder, C., Denys, G., Dettai, A., Duhamel, G., Eleaume, M., Feral, J.P., Gallut, C., Havermans, C., Held, C., Hemery, L., Lautredou, A.C., Martin, P., Ozouf-Costaz, C., Pierrat, B., Pruvost, P., Puillandre, N., Samadi, S., Saucede, T., Schubart, C., David, B., 2013. Is the species flock concept operational? The Antarctic shelf case. PloS one 8, e68787.
Lee, Y.-H., Song, M., Lee, S., Leon, R., Godoy, S.O., Canete, I., 2004. Molecular phylogeny and divergence time of the Antarctic sea urchin (*Sterechinus neumayeri*) in relation to the South American sea urchins. Antarctic Science 16, 29-36.

Lewis, A.R., Marchant, D.R., Ashworth, A.C., Hedenäs, L., Hemming, S.R., Johnson, J.V., Leng, M.J., Machlus, M.L., Newton, A.E., Raine, J.I., Willenbring, J.K., Williams, M., Wolfe, A.P., 2008. Mid-Miocene cooling and the extinction of tundra in continental Antarctica. Proceedings of the National Academy of Sciences 105, 10676-10680.
Li, S., Cordero, E.C., Karoly, D.J., 2002. Transport out of the Antarctic polar vortex from a three-dimensional transport model. Journal of Geophysical Research: Atmospheres 107, ACL 8-1-ACL 8-8.
Liow, L.H., Quental, T.B., Marshall, C.R., 2010. When can decreasing diversification rates be detected with molecular phylogenies and the fossil record? Systematic Biology 59, 646-659.
Lipps, J., Hickman, C., 1982. Origin, age, and evolution of Antarctic and deep-sea faunas.
Livermore, R., Nankivell, A., Eagles, G., Morris, P., 2005. Paleogene opening of Drake Passage. Earth and Planetary Science Letters 236, 459-470.
Lörz, A.-N., 2009. Synopsis of Amphipoda from two recent Ross Sea voyages with description of a new species of *Epimeria* (Epimeriidae, Amphipoda, Crustacea). Zootaxa 2167, 59-68.
Lörz, A.-N., Held, C., 2004. A preliminary molecular and morphological phylogeny of the Antarctic Epimeriidae and Iphimediidae (Crustacea, Amphipoda). Molecular Phylogenetics and Evolution 31, 4-15.
Lörz, A.-N., Maas, E.W., Linse, K., Coleman, C.O., 2009. Do circum-Antarctic species exist in peracarid Amphipoda? A case study in the genus *Epimeria* Costa, 1851 (Crustacea, Peracarida, Epimeriidae). Zookeys 18, 91-128.
Lörz, A.-N., Maas, E.W., Linse, K., Fenwick, G.D., 2007. *Epimeria schiaparelli* sp. nov., an amphipod crustacean (family Epimeriidae) from the Ross Sea, Antarctica, with molecular characterisation of the species complex. Zootaxa, 23-27.
Lörz, A.-N., Smith, P., Linse, K., Steinke, D., 2011. High genetic diversity within *Epimeria georgiana* (Amphipoda) from the southern Scotia Arc. Mar Biodiv 42, 137-159.
Losos, J.B., Mahler, D.L., 2010. Adaptive radiation: the interaction of ecological opportunity, adaptation, and speciation. In: M.A. Bell, D.J.F., W.F. Eanes, and J.S. Levinton (Ed.), Evolution since Darwin: the first 150 years. Sinauer Associates, Sunderland, MA, pp. 381-420.
Lyle, M., Gibbs, S., Moore, T.C., K, R.D., 2007. Late Oligocene initiation of the Antarctic Circumpolar Current: evidence from the South Pacific. Geology 35, 691-694.
Mamos, T., Wattier, R., Burzynski, A., Grabowski, M., 2016. The legacy of a vanished sea: a high level of diversification within a European freshwater amphipod species complex driven by 15 My of Paratethys regression. Molecular ecology 25, 795-810.
Matschiner, M., Hanel, R., Salzburger, W., 2011. On the origin and trigger of the notothenioid adaptive radiation. PloS one 6, e18911.
McInnes, L., Orme, C.D.L., Purvis, A., 2011. Detecting shifts in diversity limits from molecular phylogenies: what can we know? Proceedings of the Royal Society B: Biological Sciences 278, 3294-3302.
McKay, R., Naish, T., Powell, R., Barrett, P., Scherer, R., Talarico, F., Kyle, P., Monien, D., Kuhn, G., Jackolski, C., 2012. Pleistocene variability of Antarctic ice sheet extent in the Ross embayment. Quaternary Science Reviews 34, 93-112.
Miller, K.G., Browning, J.V., Aubry, M.-P., Wade, B.S., Katz, M.E., Kulpecz, A.A., Wright, J.D., 2008. Eocene–Oligocene global climate and sea-level changes: St. Stephens Quarry, Alabama. Geological Society of America Bulletin 120, 34-53.
Miller, K.G., Wright, J.D., Fairbanks, R.G., 1991. Unlocking the Ice House: Oligocene-Miocene oxygen isotopes, eustasy, and margin erosion. Journal of Geophysical Research: Solid Earth 96, 6829-6848.

Miller, M.A., Pfeiffer, W., Schwartz, T., 2010. Creating the CIPRES science gateway for inference of large phylogenetic trees. Proceedings of the Gateway Computing Environments Workshop (GCE), 1-8.
Misof, B., Misof, K., 2009. A Monte Carlo approach successfully identifies randomness in multiple sequence alignments: a more objective means of data exclusion. Systematic Biology 58, 21-34.
Morlon, H., Parsons, T.L., Plotkin, J.B., 2011. Reconciling molecular phylogenies with the fossil record. Proceedings of the National Academy of Science USA 108, 16327-16332.
Nahavandi, N., Ketmaier, V., Plath, M., Tiedemann, R., 2013. Diversification of Ponto-Caspian aquatic fauna: morphology and molecules retrieve congruent evolutionary relationships in *Pontogammarus maeoticus* (Amphipoda: Pontogammaridae). Molecular Phylogenetics and Evolution 69, 1063-1076.
Near, T.J., 2004. Estimating divergence times of notothenioid fishes using a fossil-calibrated molecular clock. Antarctic Science 16, 37-44.
Near, T.J., Dornburg, A., Kuhn, K.L., Eastman, J.T., Pennington, J.N., Patarnello, T., Zane, L., Fernández, D.A., Jones, C.D., 2012. Ancient climate change, antifreeze, and the evolutionary diversification of Antarctic fishes. Proceedings of the National Academy of Sciences USA 109, 3434-3439.
Nee, S., 2006. Birth-Death Models in Macroevolution. Annual Review of Ecology, Evolution, and Systematics 37, 1-17.
Orsi, A.H., Whitworth, T., Sparrow, M., Chapman, P., Gould, J., 2005. Hydrographic atlas of the world ocean circulation experiment (WOCE) Vol 1: Southern Ocean. WOCE International Project Office, Southhampton, UK.
Otto, J.C., Wilson, K.J., 2001. Assessment of the usefulness of ribosomal 18S and mitochondrial COI sequences in Prostigmata phylogeny. CSIRO Publishing, 150 Oxford Street, Collingwood, Victoria, Australia.
Page, T.J., Linse, K., 2002. More evidence of speciation and dispersal across the Antarctic Polar Front through molecular systematics of Southern Ocean *Limatula* (Bivalvia: Limidae). Polar Biology 25, 818-826.
Passchier, S., O'Brien, P.E., Damuth, J.E., Januszczak, N., Handwerger, D.A., Whitehead, J.M., 2003. Pliocene–Pleistocene glaciomarine sedimentation in eastern Prydz Bay and development of the Prydz trough-mouth fan, ODP Sites 1166 and 1167, East Antarctica. Marine Geology 199, 279-305.
Pawlowski, J., Fahrni, J., Lecroq, B., Longet, D., Cornelius, N., Excoffier, L., Cedhagen, T., Gooday, A.J., 2007. Bipolar gene flow in deep-sea benthic Foraminifera. Molecular ecology 16, 4089-4096.
Peck, L.S., 2002. Ecophysiology of Antarctic marine ectotherms: limits to life. In: Arntz, W.E., Clarke, A. (Eds.), Ecological Studies in the Antarctic Sea Ice Zone: Results of EASIZ Midterm Symposium. Springer Berlin Heidelberg, Berlin, Heidelberg, pp. 221-230.
Pfuhl, H.A., McCave, I.N., 2005. Evidence for late Oligocene establishment of the Antarctic Circumpolar Current. Earth and Planetary Science Letters 235, 715-728.
Phillimore, A.B., Price, T.D., 2008. Density-Dependent Cladogenesis in Birds. PLOS Biology 6, e71.
Phillimore, A.B., Price, T.D., 2009. Ecological influences on the temporal pattern of speciation. In: Butlin R., B.J., Schluter D. (Ed.), Speciation and patterns of diversity. Cambridge University Press, Cambridge, pp. 240-256.
Pilar Cabezas, M., Cabezas, P., Machordom, A., Guerra-García, J.M., 2013. Hidden diversity and cryptic speciation refute cosmopolitan distribution in *Caprella penantis* (Crustacea: Amphipoda: Caprellidae). Journal of Zoological Systematics and Evolutionary Research 51, 85-99.
Plummer, M., Best, N., Cowles, K., Vines, K., 2005. Coda: output analysis and diagnostics for MCMC. R package version 0.9-2 3.
Pollard, D., DeConto, R.M., 2009. Modelling West Antarctic ice sheet growth and collapse through the past five million years. Nature 458, 329-332.
Purvis, A., 2008. Phylogenetic approaches to the study of extinction. Annual Review of Ecology, Evolution, and Systematics 39, 301-319.

Pybus, O.G., Harvey, P.H., 2000. Testing macro-evolutionary models using incomplete molecular phylogenies. Proceedings of the Royal Society B: Biological Sciences 267, 2267-2272.
Quental, T.B., Marshall, C.R., 2009. Extinction during evolutionary radiations: reconciling the fossil record with molecular phylogenies. Evolution 63, 3158-3167.
Quental, T.B., Marshall, C.R., 2010. Diversity dynamics: molecular phylogenies need the fossil record. Trends in Ecology & Evolution 25, 434-441.
Rabosky, D.L., 2006a. LASER: a Maximum Likelihood toolkit for detecting temporal shifts in diversification rates from molecular phylogenies. Evolutionary Bioinformatics Online 2, 247-250.
Rabosky, D.L., 2006b. Likelihood methods for detecting temporal shifts in diversification rates. Evolution 60, 1152-1164.
Rabosky, D.L., 2010. Extinction rates should not be estimated from molecular phylogenies. Evolution 64, 1816-1824.
Rabosky, D.L., 2014. Automatic detection of key innovations, rate shifts, and diversity-dependence on phylogenetic trees. PloS one 9, e89543.
Rabosky, D.L., Grundler, M., Anderson, C., Title, P., Shi, J.J., Brown, J.W., Huang, H., Larson, J.G., 2014. BAMMtools: an R package for the analysis of evolutionary dynamics on phylogenetic trees. Methods in Ecology and Evolution 5, 701-707.
Rabosky, D.L., Lovette, I.J., 2008. Density-dependent diversification in North American wood warblers. Proc Biol Sci 275, 2363-2371.
Rambaut, A., Drummond, A., 2005. Tracer, a program for analyzing results from Bayesian MCMC programs such as BEAST & MrBayes, version 1.3. Oxford, online at <http://evolve/zoo.ox.ac.uk/software.html?id=tracer/>.
Rambaut, A., Suchard, M.A., Xie, D., Drummond, A.J., 2014. Tracer v1.6. Available from http://beast.bio.ed.ac.uk/Tracer.
Raupach, M.J., Malyutina, M., Brandt, A., Wägele, J.-W., 2007. Molecular data reveal a highly diverse species flock within the munnopsoid deep-sea isopod *Betamorpha fusiformis* (Barnard, 1920) (Crustacea: Isopoda: Asellota) in the Southern Ocean. Deep Sea Research Part II: Topical Studies in Oceanography 54, 1820-1830.
Ricklefs, R.E., 2007. Estimating diversification rates from phylogenetic information. Trends in Ecology & Evolution 22, 601-610.
Ricklefs, R.E., Jønsson, K.A., 2014. Clade extinction appears to balance species diversification in sister lineages of Afro-Oriental passerine birds. Proceedings of the National Academy of Sciences 111, 11756-11761.
Rogers, A.D., 2000. The role of the oceanic oxygen minima in generating biodiversity in the deep sea. Deep Sea Research Part II: Topical Studies in Oceanography 47, 119-148.
Ronquist, F., Huelsenbeck, J.P., 2003. MrBayes 3: Bayesian phylogenetic inference under mixed models. Bioinformatics 19, 1572-1574.
Rundell, R.J., Price, T.D., 2009. Adaptive radiation, nonadaptive radiation, ecological speciation and nonecological speciation. Trends in Ecology & Evolution 24, 394-399.
Sanger, F., Nicklen, S., Coulson, A.R., 1977. DNA sequencing with chain-terminating inhibitors. Proceedings of the National Academy of Science USA 74, 5463-5467.
Scher, H.D., Martin, E.E., 2004. Circulation in the Southern Ocean during the Paleogene inferred from neodymium isotopes. Earth and Planetary Science Letters 228, 391-405.
Schluter, D., 2000. The ecology of adaptive radiation. Oxford University Press, Oxford.
Shaw, P.W., Arkhipkin, A.I., Al-Khairulla, H., 2004. Genetic structuring of Patagonian toothfish populations in the Southwest Atlantic Ocean: the effect of the Antarctic Polar Front and deep-water troughs as barriers to genetic exchange. Molecular ecology 13, 3293-3303.
Shevenell, A.E., Kennett, J.P., Lea, D.W., 2004. Middle Miocene Southern Ocean cooling and Antarctic cryosphere expansion. Science 305, 1766.

Smith, W.H.F., Sandwell, D.T., 1997. Global sea floor topography from satellite altimetry and ship depth soundings. Science 277, 1956.
Sorlien, C.C., Luyendyk, B.P., Wilson, D.S., Decesari, R.C., Bartek, L.R., Diebold, J.B., 2007. Oligocene development of the West Antarctic Ice Sheet recorded in eastern Ross Sea strata. Geology 35, 467-470.
Stadler, T., 2011. Mammalian phylogeny reveals recent diversification rate shifts. Proceedings of the National Academy of Sciences of the USA 108, 6187-6192.
Stickley, C.E., Brinkhuis, H., Schellenberg, S.A., Sluijs, A., Röhl, U., Fuller, M., Grauert, M., Huber, M., Warnaar, J., Williams, G.L., 2004. Timing and nature of the deepening of the Tasmanian Gateway. Paleoceanography 19.
Strugnell, J.M., Cherel, Y., Cooke, I.R., Gleadall, I.G., Hochberg, F.G., Ibáñez, C.M., Jorgensen, E., Laptikhovsky, V.V., Linse, K., Norman, M., Vecchione, M., Voight, J.R., Allcock, A.L., 2011. The Southern Ocean: source and sink? Deep Sea Research Part II: Topical Studies in Oceanography 58, 196-204.
Strugnell, J.M., Rogers, A.D., Prodöhl, P.A., Collins, M.A., Allcock, A.L., 2008. The thermohaline expressway: the Southern Ocean as a centre of origin for deep-sea octopuses. Cladistics 24, 853-860.
Swofford, D.L., 2003. PAUP*. Phylogenetic analysis using parsimony (*and other methods). Version 4. Sinauer Associates, Sunderland, Massachusetts.
Tamura, K., Stecher, G., Peterson, D., Filipski, A., Kumar, S., 2013. MEGA6: molecular evolutionary genetics analysis version 6.0. Molecular Biology and Evolution 30, 2725-2729.
Taylor, B.J., 1972. An urdid isopod from the Lower Cretaceous of South-East Alexander Island. British Antarctic Survey Bulletin 27, 97-103.
Thatje, S., Fuentes, V., 2003. First record of anomuran and brachyuran larvae (Crustacea: Decapoda) from Antarctic waters. Polar Biology 26, 279-282.
Thatje, S., Hillenbrand, C.-D., Larter, R., 2005. On the origin of Antarctic marine benthic community structure. Trends in Ecology & Evolution 20, 534-540.
Vaidya, G., Lohman, D.J., Meier, R., 2011. SequenceMatrix: concatenation software for the fast assembly of multi-gene datasets with character set and codon information. Cladistics 27, 171-180.
Verheye, M.L., Backeljau, T., d'Udekem d'Acoz, C., 2016. Looking beneath the tip of the iceberg: diversification of the genus *Epimeria* on the Antarctic shelf (Crustacea, Amphipoda). Polar Biology 39, 925-945.
Verheye, M.L., Martin, P., Backeljau, T., D'Udekem D'Acoz, C., 2015. DNA analyses reveal abundant homoplasy in taxonomically important morphological characters of Eusiroidea (Crustacea, Amphipoda). Zoologica Scripta 45, 300-321.
Walker, T., Valentine, J., 1984. Equilibrium models of evolutionary species diversity and the number of empty niches. The American Naturalist 124, 887-899.
Warrant, E.J., Locket, N.A., 2004. Vision in the deep sea. Biological reviews of the Cambridge Philosophical Society 79, 671-712.
Waters, J.M., 2008. Driven by the West Wind Drift? A synthesis of southern temperate marine biogeography, with new directions for dispersalism. Journal of Biogeography 35, 417-427.
Waters, J.M., McCulloch, G.A., Eason, J.A., 2007. Marine biogeographical structure in two highly dispersive gastropods: implications for trans-Tasman dispersal. Journal of Biogeography 34, 678-687.
Weir, J.T., 2006. Divergent timing and patterns of species accumulation in lowland and highland neotropical birds. Evolution 60, 842-855.
Williams, S.T., Reid, D.G., Littlewood, D.T., 2003. A molecular phylogeny of the Littorininae (Gastropoda: Littorinidae): unequal evolutionary rates, morphological parallelism, and biogeography of the Southern Ocean. Molecular Phylogenetics and Evolution 28, 60-86.

Wilson, D.S., Pollard, D., DeConto, R.M., Jamieson, S.S.R., Luyendyk, B.P., 2013. Initiation of the West Antarctic Ice Sheet and estimates of total Antarctic ice volume in the earliest Oligocene. Geophysical Research Letters 40, 4305-4309.
Witt, J.D.S., Threloff, D.L., Hebert, P.D.N., 2006. DNA barcoding reveals extraordinary cryptic diversity in an amphipod genus: implications for desert spring conservation. Molecular ecology 15, 3073-3082.
Woodburne, M.O., Zinsmeister, W.J., 1984. The first land mammal from Antarctica and its biogeographic implications. Journal of Paleontology 58, 913.
Yoder, J.B., Clancey, E., Des Roches, S., Eastman, J.M., Gentry, L., Godsoe, W., Hagey, T.J., Jochimsen, D., Oswald, B.P., Robertson, J., Sarver, B.A.J., Schenk, J.J., Spear, S.F., Harmon, L.J., 2010. Ecological opportunity and the origin of adaptive radiations. Journal of Evolutionary Biology 23, 1581-1596.
Zinsmeister, W.J., 1979. Biogeographic significance of the late Mesozoic and early Tertiary molluscan faunas of Seymour Island (Antarctic Peninsula) to the final breakup of Gondwanaland. In: Gray J., B.A.J. (Ed.), Historical biogeography, plate tectonics, and the changing environment. Oregon State University Press, Corvallis, pp. 349-355.
Zinsmeister, W.J., 1984. Late Eocene bivalves (Mollusca) from the La Meseta Formation, collected during the 1974-1975 joint Argentine-American expedition to Seymour Island, Antarctic Peninsula. Journal of Paleontology, 1497-1527.
Zwickl, D.J., 2006. Genetic algorithm approaches for the phylogenetic analysis of large biological sequence datasets under the maximum likelihood criterion. Ph.D. dissertation. University of Texas, Austin.

Captions

Figure 1. Bayesian phylogenetic tree of the concatenated dataset (COI, 28S, H3). Posterior probabilities are indicated above the nodes and Bootstrap values (> 50) from the Maximum Likelihood analysis below the nodes. MOTUs names (putative species) from Verheye et al. (2016) are indicated for Antarctic *Epimeria* specimens.

Figure 2. Maximum clade credibility chronophylogenetic tree from the BEAST analysis of the concatenated dataset. Blue bars on the tree indicate 95 % confidence intervals for estimated node ages. Mean node ages are indicated in front of the bars. Posterior probabilities are indicated above the nodes. The grey shaded area is the 95 % confidence interval of the initial diversification of the Antarctic *Epimeria* clade. The paleogeographic figures (from Zinsmeister, 1982) on the tree show the Late Gondwana's breakup. Shaded area on these figures represent inferred areas of shallow marine conditions. The graph below (modified from Zachos et al. 2008) shows the paleotemperatures over the past 65 million years, inferred from the benthic foraminiferal $\delta^{18}O$ curve, which is based on records from Deep Sea Drilling Project and Ocean Drilling Program sites. EECO = Early Eocene Climate Optimum; EOCT = Eocene-Oligocene Climate Transition; MMCT = Middle Miocene Climate Transition.

Figure 3. Lineage diversification through time plot of the Antarctic *Epimeria* clade, generated with the dated tree from the BEAST analysis (in red). Dotted lines represent the 95% confidence interval of lineage diversification simulated 100 times under PB (A) and BD (B) models, with $\lambda = 0.09$ (PB) and with $\lambda = 0.09$ and $\mu = 0.02$ (BD), and assuming a sampling fraction of 0.72.

Figure 4. Net diversification rate through time inferred with BAMM for the Antarctic Epimeria clade, assuming sampling fractions of A. 0.1 B. 0.5 and C. 0.72.The shaded blue area represents the 95 % credible interval on the rate values.

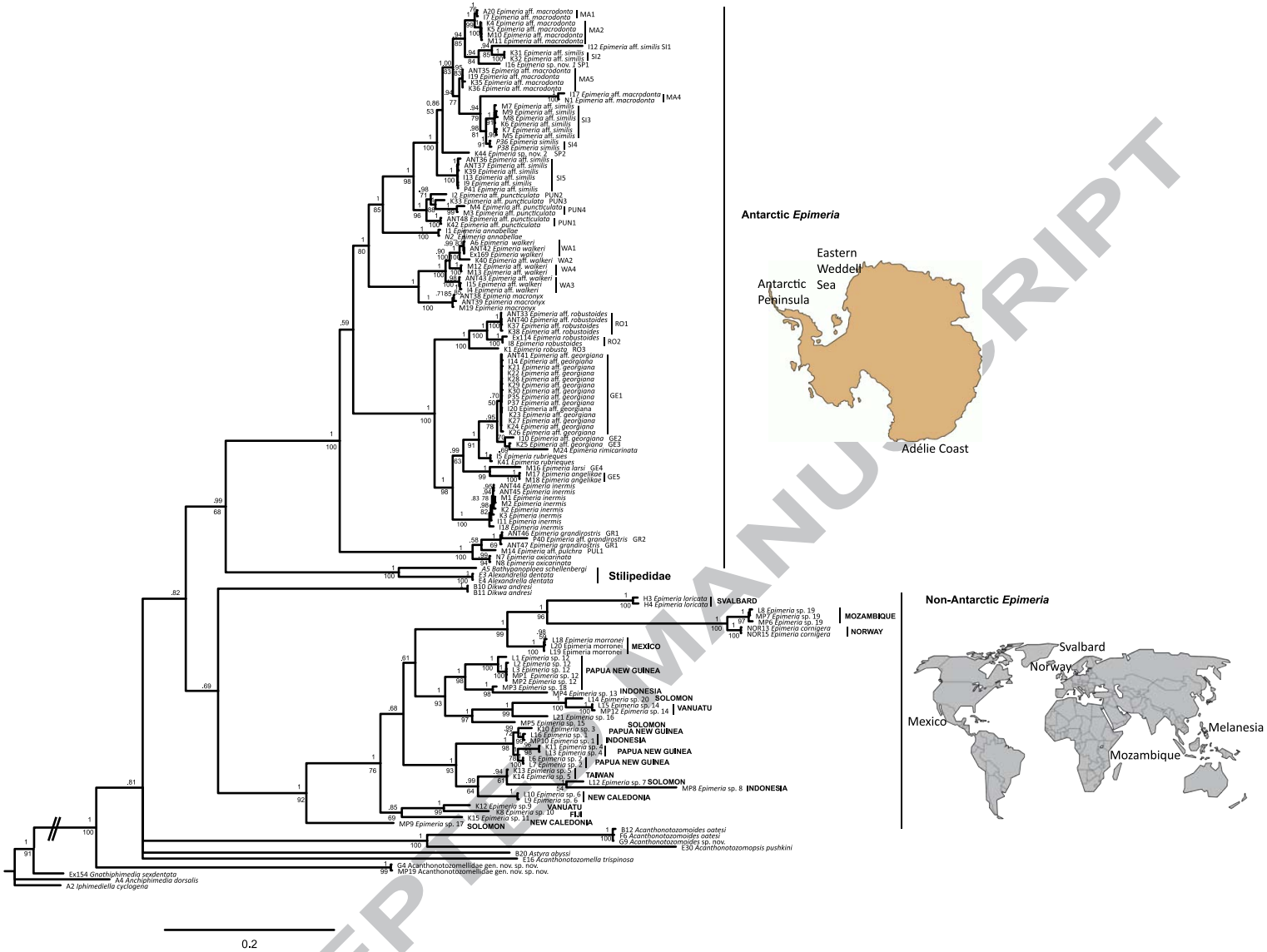

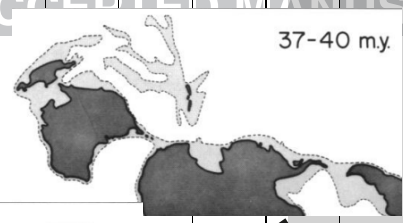

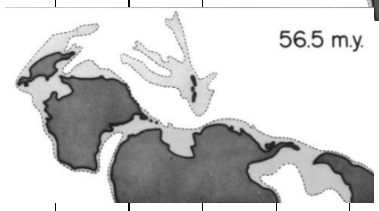

A20 *Epimeria* aff. *macrodonta* MA1
K4 *Epimeria* aff. *macrodonta* MA2
I12 *Epimeria* aff. *similis* SI1
K31 *Epimeria* aff. *similis* SI2
I16 *Epimeria* sp. nov. SP1
I17 *Epimeria* aff. *macrodonta* MA4
M7 *Epimeria* aff. *similis* SI3
P36 *Epimeria similis* SI4
I19 *Epimeria* aff. *macrodonta* MA3
ANT36 *Epimeria* aff. *similis* SI5
K44 *Epimeria* sp. nov. SP2
I2 *Epimeria* aff. *puncticulata* PUN2
K33 *Epimeria* aff. *puncticulata* PUN3
M4 *Epimeria* aff. *puncticulata* PUN4
ANT48 *Epimeria* aff. *puncticulata* PUN1
I1 *Epimeria annabellae*
A6 *Epimeria* aff. *walkeri* WA1
K40 *Epimeria* aff. *walkeri* WA2
M12 *Epimeria* aff. *walkeri* WA4
ANT43 *Epimeria* aff. *walkeri* WA3
ANT38 *Epimeria macronyx*
ANT46 *Epimeria grandirostris* GR1
P40 *Epimeria* aff. *grandirostris* GR2
M14 *Epimeria* aff. *pulchra* PUL1
N7 *Epimeria oxicarinata* OX
ANT33 *Epimeria* aff. *robustoides* RO1
Ex114 *Epimeria robustoides* RO2
K1 *Epimeria robusta* RO3
ANT41 *Epimeria* aff. *georgiana* GE1
I10 *Epimeria* aff. *georgiana* GE2
K25 *Epimeria* aff. *georgiana* GE3
M24 *Epimeria rimicarinata* RI
I5 *Epimeria rubrieques* RU
M16 *Epimeria larsi* GE4
M17 *Epimeria angelikae* GE5
ANT44 *Epimeria inermis*
A5 *Bathypanoploea schellenbergi*
E3 *Alexandrella dentata*
B10 *Dikwa andresi*
H3 *Epimeria loricata*
MP6 *Epimeria* sp. 19
NOR15 *Epimeria cornigera*
L20 *Epimeria morronei*
K10 *Epimeria* sp. 3
MP10 *Epimeria* sp.1
L13 *Epimeria* sp. 4
L7 *Epimeria* sp. 2
K14 *Epimeria* sp. 5
L12 *Epimeria* sp.7
L10 *Epimeria* sp. 6
MP8 *Epimeria* sp. 8
K12 *Epimeria* sp. 9
K8 *Epimeria* sp.10
K15 *Epimeria* sp.11
MP9 *Epimeria* sp.17
L14 *Epimeria* sp. 20
L15 *Epimeria* sp.14
L21 *Epimeria* sp.16
MP5 *Epimeria* sp.15
L2 *Epimeria* sp.12
MP3 *Epimeria* sp.18
MP4 *Epimeria* sp.13
B12 *Acanthonotozomoides oatesi*
E30 *Acanthonotozomopsis pushkini*
G4 Acanthonotozomellidae gen. nov. sp. nov.
B20 *Astyra abyssi*
E16 *Acanthonotozomella trispinosa*

8.0

125 100 75 50 25 0

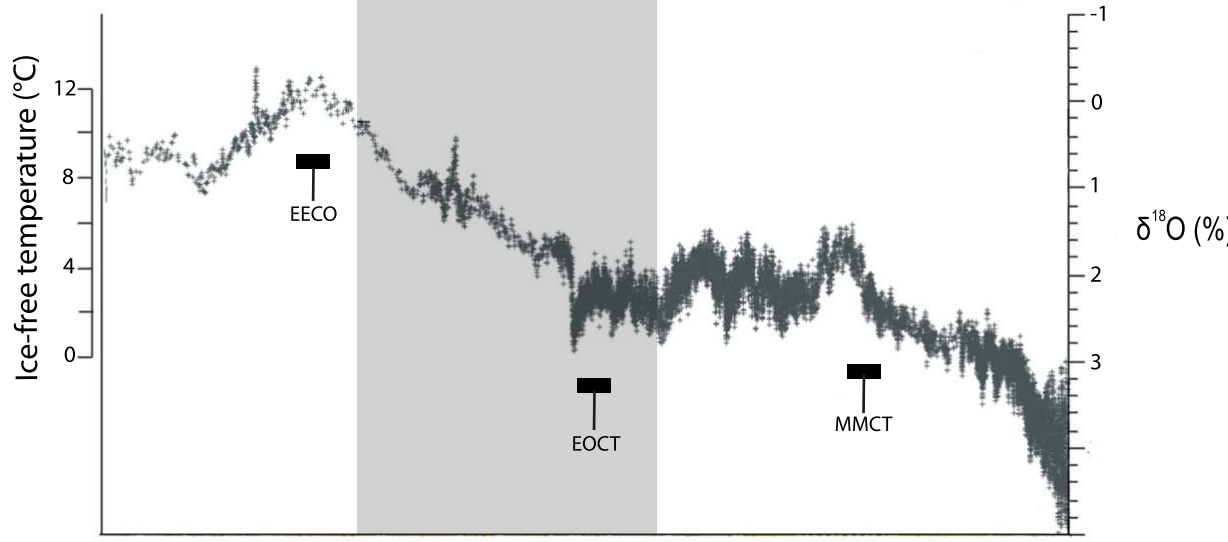

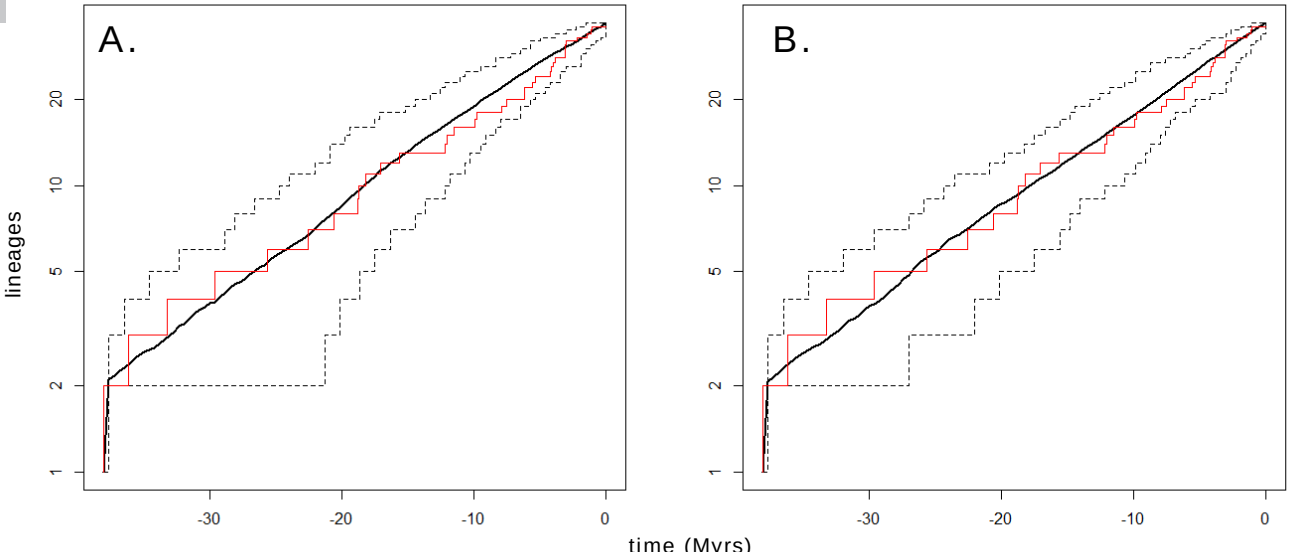
A.
B.
lineages
1
2
5
10
20
-30
-20
-10
0
time (Myrs)

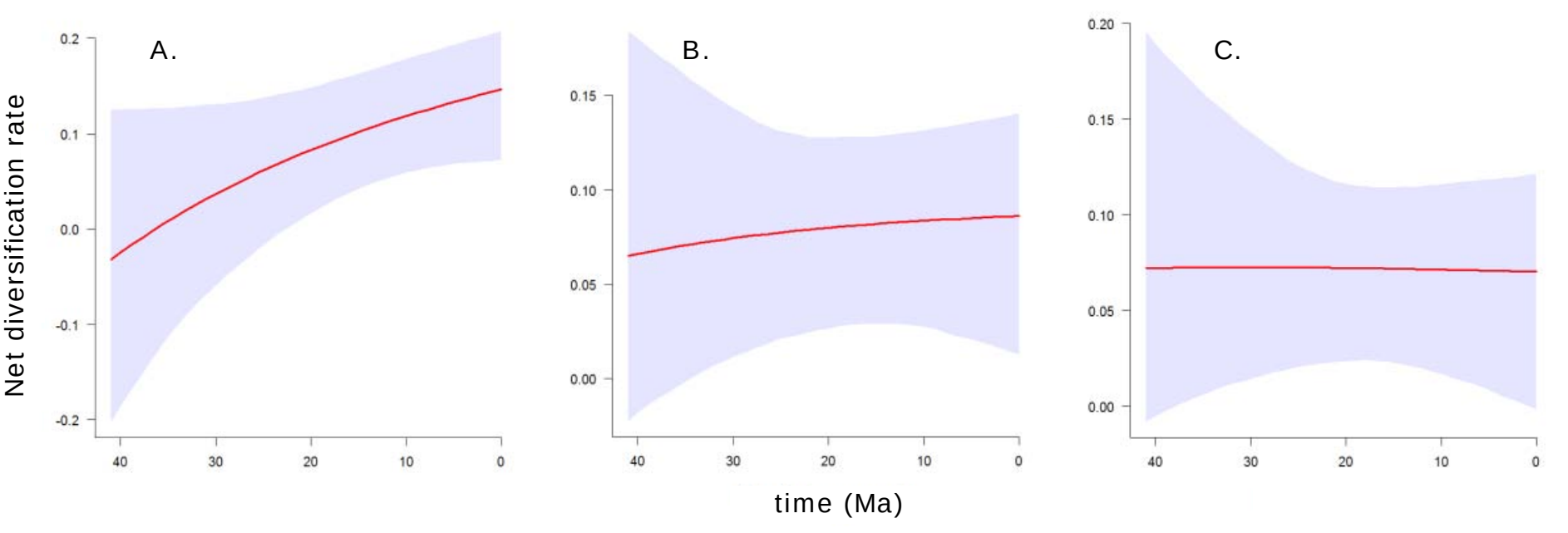
A.
B.
C.
Net diversification rate
time (Ma)
0.2
0.1
0.0
-0.1
-0.2
0.15
0.10
0.05
0.00
0.20
40
30
20
10
0

Specimens id code	Species					Genbank accession number		
		Locality	Latitude	Longitude	Voucher ID	COI	28S	H3
EPIMERIIDAE								
A20	*Epimeria* aff. *macrodonta* MA1	Peninsula, Larsen B	65° 57.51' S	60° 28.15' W	RBINS INV.132655	KU870817	KU759589	**KY825815**
I7	*Epimeria* aff. *macrodonta* MA1	Peninsula, Larsen B	65° 57.51' S	60° 28.15' W	RBINS INV.132975	KU870851	KU759628	**KY825863**
K4	*Epimeria* aff. *macrodonta* MA2	Adélie Coast	66° 38.42' S	139° 49.72’ E	MNHN-IU-2009-2570	KU870872	KU759652	**KY825893**
K5	*Epimeria* aff. *macrodonta* MA2	Adélie Coast	66° 36.37' S	140°05.07' E	MNHN-IU-2009-2563	KU870876	KU759657	**KY825898**
M10	*Epimeria* aff. *macrodonta* MA2	Adélie Coast	66° 41.12' S	139° 56.69' E	MNHN-IU-2014-4299	KU870878	KU759661	**KY825921**
M11	*Epimeria* aff. *macrodonta* MA2	Adélie Coast	66° 40.12' S	139° 55.93' E	MNHN-IU-2014-4296	N/A	KU759662	**KY825922**
I19	*Epimeria* aff. *macrodonta* MA3	Peninsula, Dundee Island	63° 37.29‘ S	56° 09.11‘ W	RBINS INV.132974	KU870844	KU759621	**KY825858**
K36	*Epimeria* aff. *macrodonta* MA3	Peninsula, North of Joinville Island	62° 33.79‘ S	56° 27.81‘ W	RBINS INV.122929B	KU87086	KU759648	**KY825889**
K35	*Epimeria* aff. *macrodonta* MA3	Peninsula, North of Joinville Island	62° 33.79‘ S	56° 27.81‘ W	RBINS INV.122929A	N/A	KU759647	**KY825888**
ANT35	*Epimeria* aff. *macrodonta* MA3	Peninsula, Erebus and Terror Gulf	63° 58.78‘ S	56° 46.24‘ W	RBINS INV.122940	N/A	KU759594	**KY825820**
I17	*Epimeria* aff. *macrodonta* MA4	Bransfield Strait East	62° 43.73‘ S	57° 29.04‘ W	RBINS INV.132660	N/A	KU759619	**KY825856**
N1	*Epimeria* aff. *macrodonta* MA4	Bransfield Strait East	62° 43.73‘ S	57° 29.04‘ W	RBINS INV.132973	N/A	KU759677	**KY825920**
I12	*Epimeria* aff. *similis* SI1	Eastern Weddell Sea	70° 50.48' S	10° 35.28' W	RBINS INV.132664	N/A	KU759614	**KY825851**
K31	*Epimeria* aff. *similis* SI2	Bransfield Strait Central	62° 53.45‘ S	58° 13.06‘ W	RBINS INV.122931A	KU870865	KU759644	**KY825885**
K32	*Epimeria* aff. *similis* SI2	Bransfield Strait Central	62° 53.45‘ S	58° 13.06‘ W	RBINS INV.122935	KU870866	KU759645	**KY825886**
K6	*Epimeria* aff. *similis* SI3	Adélie Coast	66° 38.00' S	140° 42.00' E	MNHN-IU-2009-2532	N/A	KU759658	**KY825899**
M7	*Epimeria* aff. *similis* SI3	Adélie Coast	66° 10.57' S	143° 20.75' E	MNHN-IU-2014-4342	N/A	KU759674	**KY825936**
M8	*Epimeria* aff. *similis* SI3	Adélie Coast	66° 45.14' S	145° 20.07' E	MNHN-IU-2014-4333	N/A	KU759675	**KY825937**
M9	*Epimeria* aff. *similis* SI3	Adélie Coast	66° 45.14' S	145° 20.07' E	MNHN-IU-2014-4322	N/A	KU759676	**KY825938**
M5	*Epimeria* aff. *similis* SI3	Adélie Coast	65° 59.83' S	143° 38.99' E	MNHN-IU-2014-4340	N/A	KU759672	**KY825934**

K7	*Epimeria* aff. *similis* SI3	Adélie Coast	66° 38.00' S	140° 42.00' E	MNHN-IU-2009-2539	N/A	KU759659	**KY825900**
P36	*Epimeria similis* SI4	Bransfield Strait East	62° 43.73‘ S	57° 29.04‘ W	RBINS INV.122956A	N/A	KU759680	**KY825935**
P38	*Epimeria similis* SI4	Bransfield Strait Central	62° 53.45‘ S	58° 13.06‘ W	RINBS INV.122922B	N/A	KU759682	**KY825953**
ANT37	*Epimeria* aff. *similis* SI5	Bransfield Strait East	62° 47.80‘ S	57° 05.35‘ W	RBINS INV.122942	KU870823	KU759596	**KY825822**
I13	*Epimeria* aff. *similis* SI5	Bransfield Strait East	62° 43.73‘ S	57° 29.04‘ W	RBINS INV.132976	KU870839	KU759615	**KY825852**
I9	*Epimeria* aff. *similis* SI5	Eastern Weddell Sea	70° 47.34' S	10° 40.39' W	RBINS INV.132665	KU870853	KU759630	**KY825865**
P41	*Epimeria* aff. *similis* SI5	Eastern Weddell Sea	70° 23.94' S	08° 19.14' W	RBINS INV.132977	KU870895	KU759684	**KY825955**
K39	*Epimeria* aff. *similis* SI5	Bransfield Strait Central	62° 53.45‘ S	58° 13.06‘ W	RBINS INV.122922A	KU870871	KU759651	**KY825892**
ANT36	*Epimeria* aff. *similis* SI5	Bransfield Strait East	62° 43.50‘ S	57° 27.92‘ W	RBINS INV.132666	KU870822	KU759595	**KY825821**
I16	*Epimeria* sp. nov. 1 SP1	Eastern Weddell Sea	70° 38.66' S	10° 28.16' W	RBINS INV.132667	KU870842	KU759618	**KY825855**
K44	*Epimeria* sp. nov. 2 SP2	Eastern Weddell Sea	70° 05.13' S	03° 23.50' W	RBINS INV.132663	KU870875	KU759656	**KY825897**
ANT48	*Epimeria* aff. *puncticulata* PUN1	Bransfield Strait	62° 45.05‘ S	57° 26.68‘ W	RBINS INV.122947	N/A	KU759607	**KY825832**
K42	*Epimeria* aff. *puncticulata* PUN1	Peninsula, Dundee Island	63°36.84' S	56° 10.28' W	RBINS INV.122934	N/A	KU759655	**KY825896**
I2	*Epimeria* aff. *puncticulata* PUN2	Peninsula, Larsen B	65° 57.51' S	60° 28.15' W	RBINS INV.132651	KU870845	KU759622	**KY825859**
K33	*Epimeria* aff. *puncticulata* PUN3	Adélie Coast	66° 39.3' S	139° 55.8' E	MNHN-IU-2009-2578	KU870867	KU759646	**KY825887**
M4	*Epimeria* aff. *puncticulata* PUN4	Adélie Coast	65° 48.48' S	143° 03.76' E	MNHN-IU-2014-4288	KU870888	KU759671	**KY825933**
M3	*Epimeria* aff. *puncticulata* PUN4	Adélie Coast	65° 48.48' S	143° 03.76' E	MNHN-IU-2014-4288	N/A	KU759670	**KY825932**
A6	*Epimeria walkeri* WA1	King George Island	62° 18.21' S	58° 39.90' W	RBINS INV.132667	KU870819	KU759591	**KY825818**
Ex169	*Epimeria walkeri* WA1	Eastern Weddell Sea	70° 56.40' S	10° 32.60' W	Specimen missing	KU870836	KU759610	**KY825842**
ANT42	*Epimeria walkeri* WA1	Bransfield Strait Central	62° 53.64‘ S	58° 12.52‘ W	RBINS INV.122944	KU870828	KU759601	**KY825826**
K40	*Epimeria aff. walkeri* WA2	Bransfield Strait East	62° 44.73‘ S	57° 26.79‘ W	RBINS INV.122932	KU870873	KU759653	**KY825894**
ANT43	*Epimeria aff. walkeri* WA3	Drake Passage West	62° 17.36‘ S	61° 12.06‘ W	RBINS INV.122949	KU870829	KU759602	**KY825827**
I15	*Epimeria aff. walkeri* WA3	Peninsula, South of Joinville Island	63° 50.92‘ S	55° 37.66‘ W	RBINS INV.132656	KU870841	KU759617	**KY825854**
I4	*Epimeria aff. walkeri* WA3	Elephant Island	61° 20.76' S	55° 12.14' W	RBINS INV.132959	KU870848	KU759625	**KY825861**

M12	*Epimeria aff. walkeri* WA4	Adélie Coast	66° 45.14' S	145° 20.07' E	MNHN-IU-2014-4331	KU870879	KU759663	**KY825923**
M13	*Epimeria aff. walkeri* WA4	Adélie Coast	66° 23.99' S	140° 32.35' E	MNHN-IU-2014-4336	KU870880	KU759664	**KY825924**
ANT38	*Epimeria macronyx* MX1	Drake Passage West	62° 22.65‘ S	61° 17.63‘ W	RBINS INV.122943	KU870824	KU759597	**KY907661**
ANT39	*Epimeria macronyx* MX1	Drake Passage West	62° 22.65‘ S	61° 17.63‘ W	RBINS INV.122943	KU870825	KU759598	**KY825823**
M19	*Epimeria macronyx* MX2	Adélie Coast	66° 44.86' S	145° 26.66' E	MNHN-IU-2014-4276	KU870885	KU759668	**KY825930**
ANT41	*Epimeria* aff. *georgiana* GE1	Bransfield Strait East	62° 44.73‘ S	57° 26.79‘ W	RBINS INV.122867	KU870827	KU759600	**KY825825**
I14	*Epimeria* aff. *georgiana* GE1	Drake Passage West	62° 17.36‘ S	61° 12.06‘ W	RBINS INV.132970	KU870840	KU759616	**KY825853**
I20	*Epimeria* aff. *georgiana* GE1	Peninsula, Dundee Island	63° 51.53‘ S	55° 40.74‘ W	RBINS INV.132971	KU870846	KU759623	**KY825860**
K21	*Epimeria* aff. *georgiana* GE1	Bransfield Strait West	63° 00.53‘ S	58° 35.67‘ W	RBINS INV.122926	KU870855	KU759633	**KY825874**
K22	*Epimeria* aff. *georgiana* GE1	Bransfield Strait West	63° 00.53‘ S	58° 35.67‘ W	RBINS INV.122924	KU870856	KU759634	**KY825875**
K23	*Epimeria* aff. *georgiana* GE1	Peninsula, East of Joinville Island	63° 10.57‘ S	54° 06.66‘ W	RBINS INV.122930A	KU870857	KU759635	**KY825876**
K24	*Epimeria* aff. *georgiana* GE1	Peninsula, East of Joinville Island	63° 10.57‘ S	54° 06.66‘ W	RBINS INV. 122933	KU870858	KU759636	**KY825877**
K26	*Epimeria* aff. *georgiana* GE1	Peninsula, South of Joinville Island	61° 56.05‘ S	60° 05.56‘ W	RBINS INV.122921A	KU870860	KU759638	**KY825879**
K27	*Epimeria* aff. *georgiana* GE1	Peninsula, North of Joinville Island	62° 33.79‘ S	56° 27.81‘ W	RBINS INV.122920	KU870861	KU759639	**KY825880**
K28	*Epimeria* aff. *georgiana* GE1	Peninsula, North of Joinville Island	62° 33.79‘ S	56° 27.81‘ W	RBINS INV.122920	KU870862	KU759640	**KY825881**
K29	*Epimeria* aff. *georgiana* GE1	Peninsula, Dundee Island	63° 37.28‘ S	56° 09.11‘ W	RBINS INV.122923	KU870863	KU759641	**KY825882**
K30	*Epimeria* aff. *georgiana* GE1	Peninsula, Dundee Island	63° 37.28‘ S	56° 09.11‘ W	RBINS INV.122925	KU870864	KU759643	**KY825884**
P35	*Epimeria* aff. *georgiana* GE1	Peninsula, South of Joinville Island	63° 51.34‘ S	55° 41.11‘ W	RBINS INV.122921B	KU870893	KU759679	**KY825927**
P37	*Epimeria* aff. *georgiana* GE1	Peninsula, South of Joinville Island	63° 51.34‘ S	55° 41.11‘ W	RBINS INV.122921C	KU870894	KU759681	**KY825952**
I10	*Epimeria* aff. *georgiana* GE2	South Orkney Islands	62° 53.45‘ S	58° 13.06‘ W	RBINS INV.132658	KU870838	KU759612	**KY825849**
K25	*Epimeria* aff. *georgiana* GE3	Drake Passage East	61° 56.05‘ S	60° 05.56‘ W	RBINS INV.122936	KU870859	KU759637	**KY825878**
M16	*Epimeria* aff. *georgiana* GE4	Adélie Coast	65° 43.12' S	143° 03.61' E	MNHN-IU-2014-4344	KU870882	KU759665	**KY825926**

M17	*Epimeria angelikae* GE5	Adélie Coast	65° 28.85' S	139° 24.18' E	MNHN-IU-2014-4278	KU870883	KU759666	**KY825928**
M18	*Epimeria angelikae* GE5	Adélie Coast	65° 52.74' S	144° 10.92' E	MNHN-IU-2014-4281-IO15	KU870884	KU759667	**KY825929**
M24	*Epimeria rimicarinata* RI	Prydz Bay	66° 55.75' S	74° 04.19' E	MNHN-IU-2014-4265	KU870887	N/A	N/A
I5	*Epimeria rubrieques* RU	Eastern Weddell Sea	70° 47.34' S	10° 40.39' W	RBINS, INV.132668	KU870849	KU759626	**KY825862**
K41	*Epimeria rubrieques* RU	Eastern Weddell Sea	70° 23.94' S	08° 19.14' W	RBINS INV.132643	KU870874	KU759654	**KY825895**
ANT44	*Epimeria inermis* IN1	Bransfield Strait West	62° 55.83‘ S	58° 41.09‘ W	RBINS INV.122948	KU870830	KU759603	**KY825828**
ANT45	*Epimeria inermis* IN1	Bransfield Strait West	63° 00.53‘ S	58° 35.67‘ W	RBINS INV.122945	KU870831	KU759604	**KY825829**
I18	*Epimeria inermis* IN1	Bransfield Strait Central	62° 57.22‘ S	58° 14.60‘ W	RBINS INV.132953	KU870843	KU759620	**KY825857**
I11	*Epimeria inermis* IN2	Eastern Weddell Sea	70° 48.93' S	10° 32.69' W	RBINS INV.132655	N/A	KU759613	**KY825850**
K2	*Epimeria inermis* IN2	Adélie Coast	66° 39.30' S	140° 01.60' E	MNHN-IU-2009-2531	N/A	KU759632	**KY825873**
K3	*Epimeria inermis* IN2	Adélie Coast	66° 40.50' S	139° 55.20' E	MNHN-IU-2009-2569	N/A	KU759642	**KY825883**
M1	*Epimeria inermis* IN2	Adélie Coast	66° 53.36' S	142° 38.90' E	MNHN-IU-2014-4272	KU870877	KU759660	**KY825919**
M2	*Epimeria inermis* IN2	Adélie Coast	66° 23.99' S	140° 32.35' E	MNHN-IU-2014-4338	KU870886	KU759669	**KY825931**
ANT33	*Epimeria* aff. *robustoides* RO1	Bransfield Strait East	62° 47.80‘ S	57° 05.35‘ W	RBINS INV.122937A	KU870820	KU759592	**KY825819**
ANT40	*Epimeria* aff. *robustoides* RO1	Bransfield Strait West	62° 55.83‘ S	58° 41.09‘ W	RBINS INV.122939	KU870826	KU759599	**KY825824**
K37	*Epimeria* aff. *robustoides* RO1	Bransfield Strait Central	62° 55.83‘ S	58° 41.09‘ W	RBINS INV.122927	KU870869	KU759649	**KY825890**
K38	*Epimeria* aff. *robustoides* RO1	Bransfield Strait Central	62° 55.83‘ S	58° 41.09‘ W	RBINS INV.122928	KU870870	KU759650	**KY825891**
Ex114	*Epimeria robustoides* RO2	Eastern Weddell Sea	70° 47.34' S	10° 40.39' W	RBINS-INV.122894	KU870834	KU759608	**KY825840**
I8	*Epimeria robustoides* RO2	Eastern Weddell Sea	70° 23.94' S	08° 19.14' W	RBINS INV.132969	KU870852	KU759629	**KY825864**
K1	*Epimeria robusta* RO3	Adélie Coast	66° 38.40' S	140° 01.80' E	MNHN-IU-2009-2571	KU870854	KU759631	**KY825866**
ANT46	*Epimeria grandirostris* GR1	Peninsula, Dundee Island	63° 51.34‘ S	55° 41.11‘ W	RBINS INV.122946	KU870832	KU759605	**KY825830**
ANT47	*Epimeria grandirostris* GR1	Bransfield Strait East	62° 45.05‘ S	57° 26.68‘ W	RBINS INV.122950	KU870833	KU759606	**KY825831**
P40	*Epimeria* aff. *grandirostris* GR2	Adélie Coast	66° 20.33' S	143° 41.13' E	MNHN-IU-2014-4327	N/A	KU759683	**KY825954**
M14	*Epimeria* aff. *pulchra* PUL1	Adélie Coast	65° 59.78' S	143° 02.95' E	MNHN-IU-2014-4284	KU870881	N/A	**KY825925**

N7	*Epimeria oxicarinata* OX	Elephant Island	61°20.27'S	55° 30.92' W	RBINS INV.122468	KU870891	N/A	**KY825949**
N8	*Epimeria oxicarinata* OX	Elephant Island	61° 20.33'S	55° 31.53' W	RBINS INV.122483	KU870892	N/A	N/A
I1	*Epimeria annabellae* AN	Eastern Weddell Sea	70° 48.93' S	10° 32.69' W	RBINS INV.132652	KU870837	KU759611	**KY825848**
N2	*Epimeria annabellae* AN	Eastern Weddell Sea	70° 30.99' S	08° 48.08' W	RBINS INV.122476	KU870890	KU759678	**KY825948**
L16	*Epimeria* sp. 1	Indonesia	05° 14.00' S	133° 00.00’ E	MNHN-IU-2009-2493	**KY907637**	N/A	**KY825908**
MP10	*Epimeria* sp. 1	Indonesia	05°15.00 S	133°01.00 E	MNHN-IU-2009-2491	**KY907648**	**KY907501**	**KY825939**
L6	*Epimeria* sp. 2	Papua New Guinea, Bismarck Sea, Dogreto Bay	03° 18.00' S	143° 00.00' E	MNHN-IU-2013-1583	**KY907643**	**KY907496**	**KY825915**
L7	*Epimeria* sp. 2	Papua New Guinea, Brokenwater Bay	03° 52.64’ S	144° 40.60 ‘ E	MNHN-IU-2013-11797	**KY907645**	**KY907497**	**KY825916**
K10	*Epimeria* sp. 3	Papua New Guinea	09° 06.00' S	152° 19.00' E	MNHN-IU-2009-2487	N/A	**KY907483**	**KY825867**
K11	*Epimeria* sp. 4	Papua New Guinea	04° 16.00' S	152° 18.00' E	MNHN-IU-2009-2486	**KY907627**	N/A	**KY825868**
L13	*Epimeria* sp. 4	Papua New Guinea, Solomon Sea, South East of Tuam Island	06° 04.25’ S	148° 10.42’ E	MNHN-IU-2013-18091	**KY907635**	**KY907488**	**KY825905**
K13	*Epimeria* sp. 5	Taiwan	24° 08.70’ N	122° 09.90’ E	MNHN-IU-2009-2520	**KY907629**	N/A	**KY825870**
K14	*Epimeria* sp. 5	Taiwan	24° 08.70’ N	122° 09.90’ E	MNHN-IU-2009-252	**KY907630**	**KY907484**	**KY825871**
L9	*Epimeria* sp. 6	New Caledonia	22° 23.40’ S	167° 21.60’ E	MNHN-IU-2013-1666	**KY907644**	**KY907499**	**KY825918**
L10	*Epimeria* sp. 6	New Caledonia	22° 21.80’ S	167° 20.80’ E	MNHN-IU-2011-6489	**KY907634**	**KY907486**	**KY825903**
L12	*Epimeria* sp. 7	Solomon Islands	07° 42.00' S	157° 43.00' E	MNHN-IU-2009-2504	N/A	**KY907487**	**KY825904**
MP8	*Epimeria* sp. 8	Indonesia	05° 46.00’ S	132° 10.00’ E	MNHN-IU-2009-2495	**KY907657**	N/A	**KY825946**
K12	*Epimeria* sp. 9	Vanuatu	16° 02.14' S	166° 38.39' E	MNHN-IU-2009-2514	**KY907628**	N/A	**KY825869**
K8	*Epimeria* sp. 10	Fiji Islands	17° 16.00' S	179° 35.00' W	MNHN-IU-2009-2517	**KY907632**	N/A	**KY825901**
K15	*Epimeria* sp. 11	New Caledonia	23° 54.00' S	167° 42.00' E	MNHN-IU-2007-2501	**KY907631**	N/A	**KY825872**
L1	*Epimeria* sp. 12	Papua New Guinea, Bismarck sea, West Kairiru Island	03° 21.00' S	143° 26.00' E	MNHN-IU-2013-18106	**KY907633**	**KY907485**	**KY825902**
L2	*Epimeria* sp. 12	Papua New Guinea, Woodlark Islands	09° 09.00' S	152° 18.00' E	MNHN-IU-2014-3478	**KY907640**	**KY907493**	**KY825911**
L3	*Epimeria* sp. 12	Papua New Guinea, Woodlark Islands	09° 07.00' S	152° 14.00' E	MNHN-IU-2014-4270	**KY907642**	N/A	**KY825914**
MP1	*Epimeria* sp. 12	Papua New Guinea	09° 09.00' S	152° 18.00' E	MNHN-IU-2009-2481	**KY907647**	**KY907500**	N/A

MP2	*Epimeria* sp. 12	Papua New Guinea	09° 09.00' S	152° 18.00' E	MNHN-IU-2009-2482	**KY907652**	**KY907503**	**KY825941**
MP4	*Epimeria* sp. 13	Indonesia	05° 15.00’ S	132° 59.00’ E	MNHN-IU-2009-2496	**KY907653**	N/A	**KY825943**
L14	*Epimeria* sp. 20	Solomon Islands	08° 24.40’ S	159° 22.55’ E	MNHN-IU-2009-2506	**KY907636**	**KY907489**	**KY825906**
L15	*Epimeria* sp. 14	Solomon Islands	08° 24.40’ S	159° 22.55’ E	MNHN-IU-2009-3479	**KY907649**	**KY907490**	**KY825907**
MP12	*Epimeria* sp. 14	Solomon Islands	08° 24.40’ S	159° 22.55’ E	MNHN-IU-2009-2511	**KY907650**	N/A	**KY825940**
MP5	*Epimeria* sp. 15	Solomon Islands	08° 19.60’ S	160° 01.95’ E	MNHN-IU-2009-2513	**KY907654**	**KY907505**	**KY825956**
L21	*Epimeria* sp. 16	Solomon Islands	09° 55.00’ S	161° 33.00’ E	MNHN-IU-2014-4315	N/A	**KY907495**	**KY825913**
MP9	*Epimeria* sp. 17	Solomon Islands	08° 19.60’ S	159° 22.55’ E	MNHN-IU-2009-2507	**KY907658**	N/A	**KY825947**
MP3	*Epimeria* sp. 18	Papua New Guinea	05° 40.00' S	154° 29.00' E	MNHN-IU-2011-2345	N/A	**KY907504**	**KY825942**
H3	*Epimeria loricata*	Svalbard, Erik Eriksenstrait	N/A	N/A	RBINS INV. 132637	**KY907625**	KT808709	**KY825846**
H4	*Epimeria loricata*	Svalbard, Hinlopen	N/A	N/A	RBINS INV. 138044	**KY907626**	**KY907482**	**KY825847**
L18	*Epimeria morronei*	Mexico, Pacific	23° 09.91’ N	115° 51.00’ W	None	**KY907638**	**KY907491**	**KY825909**
L19	*Epimeria morronei*	Mexico, Pacific	29° 20.90’ N	115°51.00’ W	None	**KY907639**	**KY907492**	**KY825910**
L20	*Epimeria morronei*	Mexico, Pacific	30° 48.40’ N	116° 47.80’ W	None	**KY907641**	**KY907494**	**KY825912**
L8	*Epimeria* sp. 19	Mozambique	24° 22.29’ S	35° 41.86’ E	MNHN-IU-2009-22	**KY907646**	**KY907498**	**KY825917**
MP6	*Epimeria* sp. 19	Mozambique, Vizconde de Eza	24° 02.06’ S	35° 40.66’ E	MNHN-IU-2009-2527	**KY907655**	N/A	N/A
MP7	*Epimeria* sp. 19	Mozambique, Visconde de Eza	24° 05.28’ S	35° 41.73’ E	MNHN-IU-2009-2525	**KY907656**	**KY907506**	**KY825945**
NOR13	*Epimeria cornigera*	Norway	68° 11.27' N	14° 59.87' E	RBINS INV. 138043	**KY907659**	**KY907507**	**KY825950**
NOR15	*Epimeria cornigera*	Norway	N/A	N/A	RBINS INV. 132630	**KY907660**	KT808708	**KY825951**
ACANTHONOTOZOMELLIDAE								
B12	*Acanthonotozomoides oatesi*	Sub-Antarctic, Shag Rocks	53° 24.81' S	42° 40.03' W	RBINS INV. 132669	**KY907616**	KT808686	**KY825834**
F6	*Acanthonotozomoides oatesi*	Sub-Antarctic, Shag Rocks	53° 23.94' S	42° 40.10' W	RBINS INV. 138046	**KY907622**	**KY907480**	**KY825843**
G9	*Acanthonotozomoides oatesi*	Sub-Antarctic, Shag Rocks	53° 24.53' S	42° 40.70' W	RBINS INV. 138045	**KY907624**	**KY907481**	**KY825845**
MP19	Acanthonotozomellidae n. gen. n. sp.	New Caledonia	23° 43.00' S	168° 02.00' E	MNHN-IU-2009-2499	**KY907651**	**KY907502**	N/A
G4	Acanthonotozomellidae n. gen. n. sp.	New Caledonia	23° 22.76' S	167° 51.60' E	MNHN-IU-2009-2497	**KY907623**	KT808685	**KY825844**
E16	*Acanthonotozomella trispinosa*	Antarctica, Larsen B	65° 57.51' S	60° 28.15' W	RBINS INV. 132673	**KY907618**	KT808684	**KY825836**
DIKWIDAE								
B10	*Dikwa andresi*	Sub-Antarctic, Burdwood Bank	54° 34.04' S	56° 10.64' W	RBINS INV. 132666	**KY907614**	**KY907478**	**KY825833**

B11	*Dikwa andresi*	Sub-Antarctic, Burdwood Bank	54° 34.04' S	56° 10.64' W	RBINS INV. 132666	**KY907615**	KT808704	N/A
STILIPEDIDAE								
A5	*Bathypanoploea schellenbergi*	Antarctica, Eastern Weddell Sea	70° 23.94' S	08° 19.14' W	RBINS INV. 132623	**KY907613**	KT808699	**KY825817**
E3	*Alexandrella dentata*	Antarctica, Eastern Weddell Sea	70° 56.52' S	10° 34.84' W	RBINS INV. 132653	**KY907619**	**KY907479**	**KY825837**
E4	*Alexandrella dentata*	Antarctica, Larsen A	64° 54.75' S	60° 39.01' W	RBINS INV. 132653	**KY907621**	KT808688	**KY825839**
B20	*Astyra abyssi*	Norway, Vestfjorden	68° 11.27' N	14° 59.87' E	RBINS INV. 132658	**KY907617**	KT808694	**KY825835**
VICMUSIIDAE								
E30	*Acanthonotozomopsis pushkini*	Sub-Antarctic, Shag Rocks	53° 24.53' S	42° 40.70' W	RBINS INV. 132656	**KY907620**	KT808687	**KY825838**
OUTGROUP								
Ex154	*Gnathiphimedia sexdentata*	Eastern Weddell Sea	70° 50.64' S	10° 36.11' W	RBINS INV.132752	KU870835	KU759609	**KY825841**
A4	*Anchiphimedia dorsalis*	Antarctica, King George Island	62° 18.21' S	58° 39.90' W	RBINS INV. 132625	**KY907612**	KT808690	**KY825816**
A2	*Iphimediella cyclogena*	Antarctica, Larsen A	64° 55.58' S	60° 33.37' W	RBINS INV. 132632	**KY907611**	KT808722	**KY825814**

Table 1. Sampling details for the sequenced *Epimeria* specimens including sample location, geographical coordinates, voucher number and GenBank accession number. "N/A" (not available) indicates unobtainable data. GenBank accession numbers of sequences obtained in this study were indicated in bold.

Table A1. Mean parameter estimates (with standard deviations) and comparison of the fit of different lineage diversification models to the empirical and semi-empirical datasets (assuming 10 %, 50 % and 72 % sampling). LH is the log-likelihood value of the model; the shift times (Ma) are indicated for the models implying discrete shifts in diversification rates; λ is the speciation rate for the constant-rate models and the initial speciation rate for the rate-variable models; μ is the extinction rate; x is the rate change parameter of the density-dependent exponential (DDX) model; K is the carrying capacity parameter of the density-dependent linear (DDL) model. For each model, the Akaike Information Criterion (AIC) was computed. The best-fitting model with the lowest AIC score is highlighted in dark grey. The 95 % confidence intervals of the AIC values are indicated. dAIC is the difference between the AIC score of the model and the AIC score of the best fitting model. Minimal and maximal values for dAIC were calculated based on the AIC 95% confidence intervals. The best-fitting model with the lowest mean AIC score is highlighted in dark grey. The evaluated models for which the dAIC range contains zero are highlighted in light grey. wAIC are the Akaike weights.

Dataset	Model	LH	Rate shift times	λ	μ	x	K	AIC	dAIC	wAIC
Semi-emp 10 %	PB	1010 (17.79)	-	0.34 (0.02)	-	-	-	-2018 (35.58) [-2022.93 ;-2013.07]	128.13 (117.25 ; 139.01)	$9\ 10^{-29}$
	BD	1075.07 (21.46)	-	0.83 (0.07)	0.74 (0.08)	-	-	-2146.13 (42.92) [-2152.08 ; -2140.18]	0.00	0.62
	DDL	1008.87 (19.75)	-	0.34 (0.02)	-	-	6085859 (1026968)	-2013.74 (39.5) [-2019.21 ; -2008.27]	132.39 (120.97 ; 143.81)	$1\ 10^{-29}$
	DDX	1073.7 (21.54)	-	0.02 (0.01)	-	-0.58 (0.05)	-	-2143.4 (43.08) [-2149.37 ; -2137.43]	2.73 (-9.19 ; 14.65)	0.16
	Yule2rate	1063.62 (20.5)	0.01 (0.01)	0.34 (0.02) 0.81 (0.61)	-	-	-	-2121.25 (41) [-2126.93 ; -2115.57]	24.88 (13.95 ; 25.85)	$2\ 10^{-6}$
	BD- 1 shift	1077.7 (21.39)	19.45 (4.86)	0.16 (0.04) 0.8 (0.08)	0.01 (0.04) 0.68 (0.11)	-	-	-2142.26 (43.08) [-2148.23 ; -2136.29]	3.87 (-8.05; 15.79)	0.09
	BD- 2 shifts	1077.92 (21.45)	19.23 (6.04) 7.63 (5.13)	0.13 (0.06) 0.7 (0.75) 0.78 (0.09)	0 (0.01) 0.52 (0.75) 0.61 (0.17)	-	-	-2139.83 (42.89) [-2145.77 ; -2133.89]	6.3 (-5.59 ; 18.19)	0.03
	BD- 3 shifts	1079.28 (21.5)	21.69 (5.18) 12.79 (7.04) 6.5 (5.59)	0.12 (0.06) 0.38 (0.02) 0.62 (0.5) 0.78 (0.09)	0 (0.01) 0.14 0.45 (0.54) 0.6 (0.2)	-	-	-2142.57 (43) [-2148.53 ; -2136.61]	3.56 (-8.35 ; 15.47)	0.10
Semi-emp 50 %	PB	14.58 (3.36)	-	0.12 (0.01)	-	-	-	-27.16 (6.73) [-28.09 ; -26.23]	0.97 (-0.99 ; 2.93)	0.17
	BD	15.88 (3.89)	-	0.16 (0.02)	0.08 (0.03)	-	-	-27.76 (7.77) [-28.84 ; -26.68]	0.37 (-1.74 ; 2.48)	0.22
	DDL	14.57 (3.38)	-	0.12 (0.01)	-	-	1202874 (229958.4)	-25.14 (6.75) [-26.07 ; -24.20]	4.88 (1.03 ; 4.96)	0.06
	DDX	15.86 (3.83)	-	0.06 (0.01)	-	-0.21 (0.07)	-	-27.73 (7.67) [-28.79 ; -26.67]	2.29 (-1.69 ; 2.49)	0.22

	Yule2rate	17.06 (3.72)	0.35 (0.21)	0.12 (0.01) 0.12 (0.1)	-	-	-	-28.13 (7.43) [-29.16 ; -27.10]	0.00	0.27
	BD- 1 shift	17.36 (3.79)	15.35 (4.61)	0.07 (0.03) 0.14 (0.02)	0.01 (0.02) 0.02 (0.03)			-24.73 (7.57) [-25.78 ; -23.68]	3.4 (1.32 ; 5.48)	0.05
	BD- 2 shifts	18.6 (3.71)	17.69 (4.64) 10.31 (6.95)	0.07 (0.02) 0.13 (0.14) 0.13 (0.03)	0 (0) 0.05 (0.14) 0.02 (0.05)	-	-	-21.19 (7.41) [-22.22 ; -20.16]	6.94 (4.88 ; 9)	$8\ 10^{-3}$
	BD- 3 shifts	19.59 (3.71)	8.09 (6.63) 14.13 (6.33) 20.43 (5.94)	0.07 (0.03) 0.16 (0.28) 0.14 (0.19) 0.13 (0.04)	0 (0) 0.06 (0.26) 0.09 (0.5) 0.03 (0.1)	-	-	-17.19 (7.42) [-18.22 ; -16.16]	10.94 (8.88 ; 13)	$1\ 10^{-3}$
Semi-emp 72 %	PB	-16.9 (1.93)	-	0.09 (0)	-	-	-	35.79 (3.85) [35.26 ; 36.32]	0.00	0.33
	BD	-16.71 (2.07)	-	0.11 (0.01)	0.02 (0.02)	-	-	37.43 (4.14) [36.86 ; 38.00]	1.64 (0.54 ; 2.74)	0.15
	DDL	-16.87 (1.9)	-	0.1 (0.01)	-	-	506016 (454041.2)	37.74 (3.8) [37.21 ; 38.27]	1.95 (0.89 ; 3.01)	0.13
	DDX	-16.71 (2.06)	-	0.07 (0.01)	-	-0.09 (0.06)	-	37.42 (4.13) [36.85 ; 37.99]	1.63 (0.53 ; 2.73)	0.15
	Yule2rate	-15.41 (1.94)	0.9 (0.3)	0.1 (0) 0.06 (0.04)	-	-		36.82 (3.88) [36.28 ; 37.36]	1.03 (-0.04 ; 2.1)	0.20
	BD- 1 shift	-15.32 (2.05)	4.73 (4.67)	0.07 (0.03) 0.09 (0.03)	0 (0.01) 0 (0)	-	-	40.64 (4.1) [40.07 ; 41.21]	4.85 (3.75 ; 5.95)	0.03
	BD- 2 shifts	-14.02 (2.01)	19.01 (4.48) 8.65 (7.99)	0.06 (0.02) 0.09 (0.08) 0.07 (0.03)	0 (0) 0.01 (0.03) 0 (0.01)	-	-	44.04 (4.01) [43.48 ; 44.59]	8.25 (7.16 ; 9.33)	$5\ 10^{-3}$
	BD- 3 shifts	-13.19 (1.93)	21.39 (5.46) 17.23 (5.96) 7.41 (7.57)	0.06 (0.03) 0.06 (0.09) 0.11 (0.08) 0.07 (0.03)	0 (0) 0.01 (0.03) 0.01 (0.07) 0 (0.01)	-	-	48.39 (3.86) [47.85 ; 48.92]	12.6 (11.53 ; 13.66)	$6\ 10^{-4}$
Empirical	PB	-28.47	-	0.078	-	-	-	58.94	0.00	0.31
	BD	-28.47	-	0.078	0.000	-	-	60.94	2.00	0.12
	DDL	-28.31	-	0.093	-	-	120.040	60.62	1.68	0.14
	DDX	-28.47	-	0.082	-	0.016	-	60.94	2.00	0.12
	Yule2rate	-26.62	2.09	0.088 0.027	-	-	-	59.24	0.30	0.27

	BD- 1 shift	-26.79	2.00	0.088 0.029	0.001 0.000	-	-	63.58	4.64	0.03
	BD- 2 shifts	-25.51	17.00 2.00	0.049 0.102 0.028	0.000 0.000 0.000	-	-	67.02	8.08	0.005
	BD- 3 shifts	-24.77	19.00 17.00 2.00	0.058 0.000 0.103 0.029	0.000 0.000 0.001 0.000	-	-	71.54	12.60	0.001

Table A2. Parameter estimates and comparison of the fit of the lineage diversification models from Morlon et al. (2011) to the empirical dataset, assuming sampling fractions of 0.72, 0.5 and 0.1. λ is the speciation rate (when constant) or the initial speciation rate (when variable); α is the rate change parameter for the exponential variation of the speciation rate; μ is the extinction rate (when constant) or the initial extinction rate (when variable) ; β is the rate change parameter for the exponential variation of the extinction rate. For each model, the Akaike Information Criterion (AIC) was computed. dAIC is the difference between the AIC score of the evaluated model and the AIC score of the best-fitting model. wAIC is the Akaike weight. The best-fitting model with the lowest AIC score is highlighted in dark grey. When the wAIC of the best model < 0.5, the second best-fit is highlighted in light grey.

Dataset	Model	AIC	dAIC	wAIC	λ	α	μ	β
Sampling 72 %	BcstDcst	245.55	2.11	0.16	0.10	-	0.02	-
	BvarDcst	247.26	3.82	0.07	0.11	-0.015	0.00	-
	BcstDvar	247.08	3.64	0.07	0.10	-	0.007	0.08
	BvarDvar	249.62	6.18	0.02	0.10	0.002	0.008	0.08
	Bcst	243.44	0.00	0.45	0.093	-	-	-
	Bvar	244.88	1.44	0.22	0.11	-0.015	-	-
Sampling 50 %	BcstDcst	245.55	1.37	0.16	0.15	-	0.07	-
	BvarDcst	246.57	2.39	0.10	0.14	-0.03	0.00	-
	BcstDvar	246.65	2.47	0.09	0.14	-	0.02	0.06
	BvarDvar	249.07	4.89	0.03	0.14	-0.02	0.004	0.07
	Bcst	244.34	0.16	0.30	0.11	-	-	-
	Bvar	244.18	0.00	0.32	0.14	-0.03	-	-
Sampling 10 %	BcstDcst	245.55	2.83	0.13	0.75	-	0.66	-
	BvarDcst	245.11	2.39	0.16	0.37	-0.07	0.00	-
	BcstDvar	245.93	3.21	0.11	0.55	-	0.39	0.01
	BvarDvar	247.59	4.87	0.05	0.42	-0.06	0.09	-0.05
	Bcst	259.60	16.88	0.00	0.19	-	-	-
	Bvar	242.72	0.00	0.54	0.37	-0.07	-	-

Highlights

- A molecular phylogeny of *Epimeria* amphipods from every world's oceans is provided.
- Antarctic and non-Antarctic *Epimeria* form 2 distinct clades.
- The Antarctic clade arose from a Late Gondwanan ancestor.
- The diversification of the Antarctic *Epimeria* clade appears related to cold-waters.

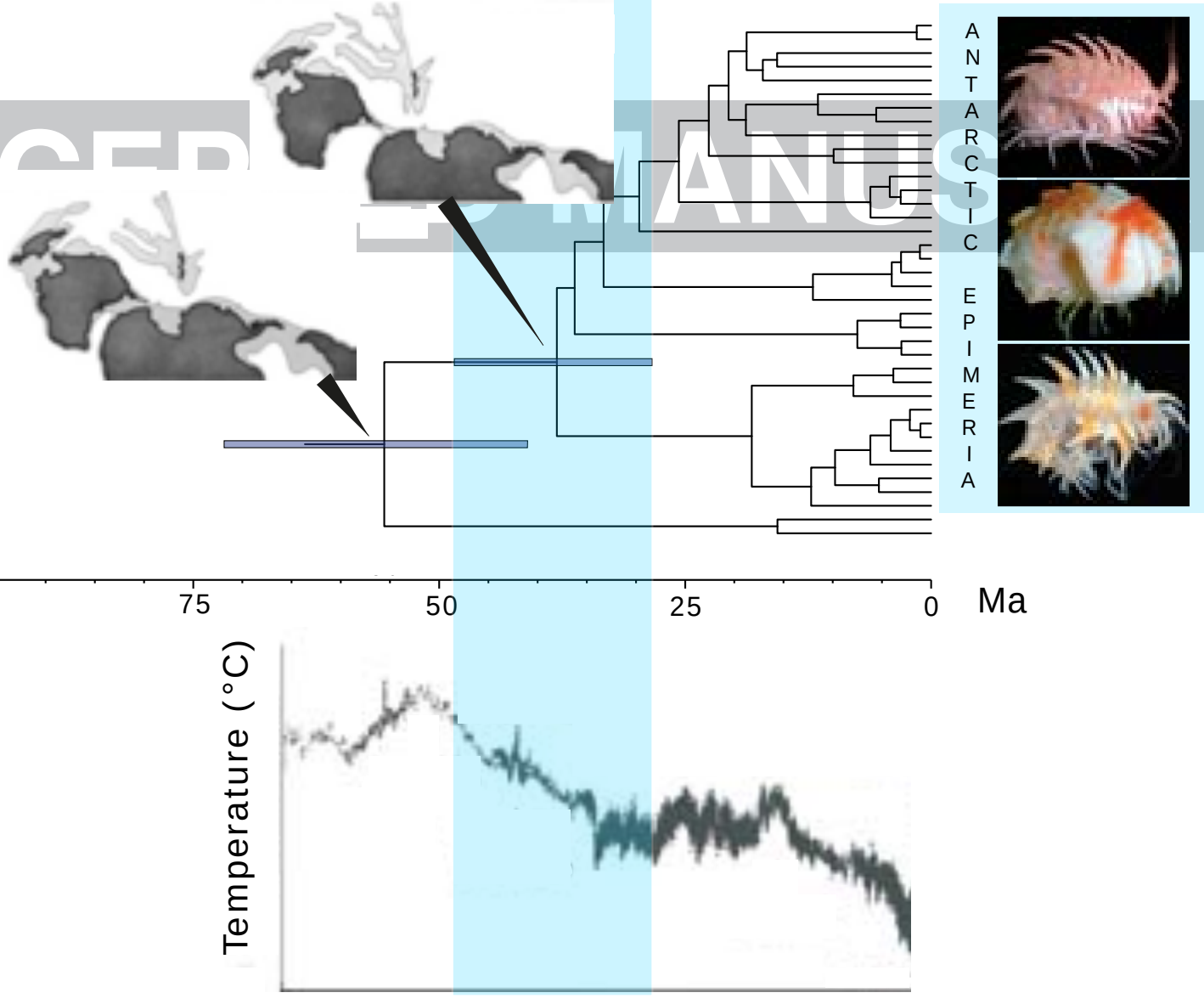
ANTARCTIC EPIMERIA
75
50
25
0
Ma
Temperature (°C)